



**ORKUSTOFNUN**

Vatnamælingar

## Mass balance modeling of the Hofsjökull ice cap based on data from 1988–2004

**Tómas Jóhannesson  
Oddur Sigurðsson  
Bergur Einarsson  
Thorsteinn Thorsteinsson**

*Prepared for the CWE, CE, VVO and VO projects*

**OS-2006/004**



**ORKUSTOFNUN**

Hydrological Service Division

## Mass balance modeling of the Hofsjökull ice cap based on data from 1988–2004

**Tómas Jóhannesson<sup>1</sup>, Oddur Sigurðsson<sup>2</sup>,  
Bergur Einarsson<sup>2</sup> and Thorsteinn Thorsteinsson<sup>2</sup>**

<sup>1</sup>Icelandic Meteorological Office

<sup>2</sup>National Energy Authority, Hydrological Service Division

*Client:*

*The CWE, CE, VVO and VO projects*

**OS-2006/004**


9979-68-180-2





# ORKUSTOFNUN

Hydrological Service Division

<b>Report no.:</b> OS-2006/004	<b>Date:</b> 17.2.2006	<b>Distribution:</b> Open <input checked="" type="checkbox"/> Closed <input type="checkbox"/> <b>Conditions:</b>
<b>Title / Main and sub-title:</b> Mass balance modeling of the Hofsjökull ice cap based on data from 1988–2004		<b>Number of copies:</b> 40 <b>Number of pages:</b> 53
<b>Authors:</b> Tómas Jóhannesson <sup>1</sup> , Oddur Sigurðsson <sup>2</sup> , Bergur Einarsson <sup>2</sup> and Thorsteinn Thorsteinsson <sup>2</sup>  <sup>1</sup> Icelandic Meteorological Office <sup>2</sup> National Energy Authority, Hydrological Service Division		<b>Project manager:</b> Tómas Jóhannesson Árni Snorrason  <b>Project number:</b> 7-692925
<b>Client:</b> The CWE, CE, VVO and VO projects		
<b>Abstract:</b> <p>A degree-day mass balance model for the Hofsjökull ice cap, central Iceland, has been derived based on mass balance measurements from the period 1988–2004. The model calibration is tested by deriving separate sets of model coefficients for subsets of the data. The calibration is found to be stable over the measurement period and for subsets from warm and cold years. The model is also tested by computing the average specific mass balance for the main ice flow basins of the ice cap for the period 1981–2000, when the ice cap is believed to have been relatively close to an equilibrium. The model is used to estimate seasonal precipitation at the locations of the mass balance stakes, which can, together with similar data from the other Icelandic ice caps, be used to calibrate a precipitation model for the Icelandic highland.</p> <p>An increase in glacier runoff is one of the most important hydrological consequences of future climate changes in Iceland. The expected runoff increase may, for example, have practical implications for the design and operation of hydroelectric power plants. The mass balance model for Hofsjökull is used to simulate changes in glacial runoff due to possible changes in future climate based on the CWE-NCS climate change scenario. About 20 years from now, annual average runoff from the area that is presently covered by ice is projected to have increased by approximately <math>0.6\text{--}0.7\text{ m a}^{-1}</math> with respect to the period 1981–2000. This corresponds to about 25% of annual average runoff in 1981–2000.</p>		
<b>Keywords:</b> Hofsjökull glacier-mass-balance mass-balance modeling climate-change-scenarios mass-balance-sensitivity		<b>ISBN-number:</b> 9979-68-180-2 <b>Signature of project manager:</b>  <b>Checked by:</b>



## **Contents**

<b>1</b>	<b>Introduction</b>	<b>7</b>
<b>2</b>	<b>The mass balance data set</b>	<b>7</b>
<b>3</b>	<b>The map of the ice cap</b>	<b>9</b>
<b>4</b>	<b>The MBT mass balance model</b>	<b>10</b>
<b>5</b>	<b>Calibration of the mass balance model</b>	<b>11</b>
<b>6</b>	<b>Average mass balance of ice flow basins</b>	<b>14</b>
<b>7</b>	<b>Stability of the model calibration</b>	<b>18</b>
<b>8</b>	<b>Comparison of different model types</b>	<b>20</b>
<b>9</b>	<b>Back-calculation of precipitation at stake locations</b>	<b>21</b>
<b>10</b>	<b>The climate scenario</b>	<b>23</b>
<b>11</b>	<b>Observed temperature changes in Iceland</b>	<b>30</b>
<b>12</b>	<b>Changes in mass balance</b>	<b>34</b>
<b>13</b>	<b>Static sensitivity of mass balance to climate changes</b>	<b>34</b>
<b>14</b>	<b>Changes in glacial runoff</b>	<b>36</b>
<b>15</b>	<b>Discussion</b>	<b>37</b>
<b>16</b>	<b>Acknowledgements</b>	<b>38</b>
<b>17</b>	<b>References</b>	<b>38</b>
<b>A</b>	<b>Appendix: Man-pages for the MBT mass balance model</b>	<b>42</b>

## List of Tables

1	Fixed model parameters. . . . .	12
2	Optimised model parameters. . . . .	13
3	Simulated net mass balance for ice flow basins on the Hofsjökull ice cap 1981–2000. . . . .	17
4	Model parameters estimated from subsets of the mass balance data. . . . .	19
5	Static sensitivity of the mass balance of Hofsjökull. . . . .	36

## List of Figures

1	Map of the Hofsjökull ice cap. . . . .	8
2	Observed winter and summer balance. . . . .	9
3	Modeled and measured winter and summer balance. . . . .	14
4	Simulated net mass balance of Hofsjökull, 1981–2000. . . . .	15
5	Simulated annual precipitation on Hofsjökull, 1981–2000. . . . .	16
6	Residual variance of different model types. . . . .	20
7	The CWE-NCS temperature change scenario, 1990–2050. . . . .	24
8	The CWE-NCS precipitation change scenario, 1990–2050. . . . .	25
9	The five ACIA model average projected temperature change from 1981–2000 to 2071–2090. . . . .	26
10	The five ACIA model average projected relative precipitation change from 1981–2000 to 2071–2090. . . . .	27
11	The monthly CWE-NCS temperature and precipitation change scenarios near Iceland. . . . .	27
12	The monthly average temperature and precipitation change near Iceland for the 5 ACIA OAGCM models. . . . .	28
13	Seasonal temperature variation at Hveravellir, 1987–2003. . . . .	29
14	Annual mean temperature in Reykjavík, 1866–2004. . . . .	30
15	Annual and seasonal warming in Reykjavík for four time periods. . . . .	31
16	Annual and seasonal warming at four meteorological stations, 1981–2004. . . . .	32
17	Annual and seasonal warming, 1981–2004, five station average. . . . .	33
18	Simulated change in net mass balance of Hofsjökull for a warming of 1°C. . . . .	35
19	Simulated monthly average runoff from Hofsjökull . . . . .	37

# 1 Introduction

Global warming during the next decades due to increasing concentrations of CO<sub>2</sub> and other trace gases in the atmosphere (IPCC, 1990, 1996, 2001) is expected to have pronounced effects on glaciers and ice caps and lead to major runoff changes from glaciated areas. Many glaciers and ice caps are projected to almost disappear during the next 100–200 years. These changes may have both local and global implications, such as changes in the discharge of glacial rivers (Hock *et al.*, 2005), changes in the vertical stratification in the upper layers of the Arctic Ocean (Curry *et al.*, 2003) and a rise in global sea level (Church *et al.*, 2001).

Effect of future climate changes on the mass balance and runoff from the Hofsjökull ice cap, central Iceland, was considered in the Nordic research project *Climate Change and Energy Production* (CCEP) (Sælthun *et al.*, 1998; Jóhannesson *et al.*, 1993, 1995a,b; Jóhannesson, 1997) based on mass balance measurements carried out by the Hydrological Service Division of the National Energy Authority (NEA) during the years 1988–1992. As a part of the Nordic research projects *Climate, Water and Energy* (CWE, “<http://www.os.is/cwe>”) and *Climate and Energy* (CE, “<http://www.os.is/ce>”), and their Icelandic counterparts *Veðurfar, vatn og orka* and *Veðurfar og orka* (VVO and VO, “<http://www.os.is/vvo>”), a new mass balance model for Hofsjökull has been calibrated based on mass balance measurements up to and including the mass balance year 2003/2004 (Sigurðsson, 1989–2004), a total of 17 mass balance years. This mass balance model has been used within CWE/CE/VVO/VO as a part of dynamic modeling of the glacier for assessing the time-dependent reduction in ice volume caused by climate warming (Aðalgeirsdóttir, 2003; Jóhannesson *et al.*, 2004). This report describes the development of the mass balance model, the definition of climate change scenarios for glacier modeling in the Icelandic highland based on the CWE-NCS climate change scenario for the Nordic countries (Räsänen, 2003; Rummukainen *et al.*, 2003), and the results of mass balance modeling for four scenarios for changes in temperature and precipitation that represent different possibilities for the development of the climate of Iceland during the 21<sup>st</sup> century.

## 2 The mass balance data set

The mass balance data set from the Hofsjökull ice cap consists of observations from the outlet glaciers Sátujökull, Þjórsárjökull and Blágnípujökull from the period 1988 to 2004 carried out by the National Energy Authority (Sigurðsson, 1989–2004). The stake network is shown in Figure 1. The winter balance is typically measured in early May and the summer balance in late September. The measured winter mass balance at the stakes is in many cases, especially in the ablation area of Sátujökull, augmented with snow thickness measurements that are carried out by manual probing down to the previous late summer or fall surface (ice in the ablation area) between the stake locations and also to the sides of the main stake lines.

Measurements at some stakes are missing in some years and the mass balance values measured at the individual stakes may contain fluctuations due to local conditions that are not considered representative for the elevation range where the stake is located. The winter and summer measurements of each mass balance year from each outlet glacier are interpreted in terms of mass balance as a unique function of elevation over the entire elevation range of the respective glacier. The interpreted values are used to estimate the specific winter, summer and annual mass balance for the three monitored ice flow basins on the ice cap in the annual mass balance reports. These interpreted data are the main data for the modeling described in this report, although the raw measurements at the stakes are also used for comparison. For the purpose of the modeling, the interpreted mass balance values are assumed to correspond to specific locations along lines down each glacier (shown in Fig. 1 as red lines), although the interpreted mass balance values are originally only considered functions of elevation within each of the three monitored ice flow basin and not tied to locations on the ice cap.



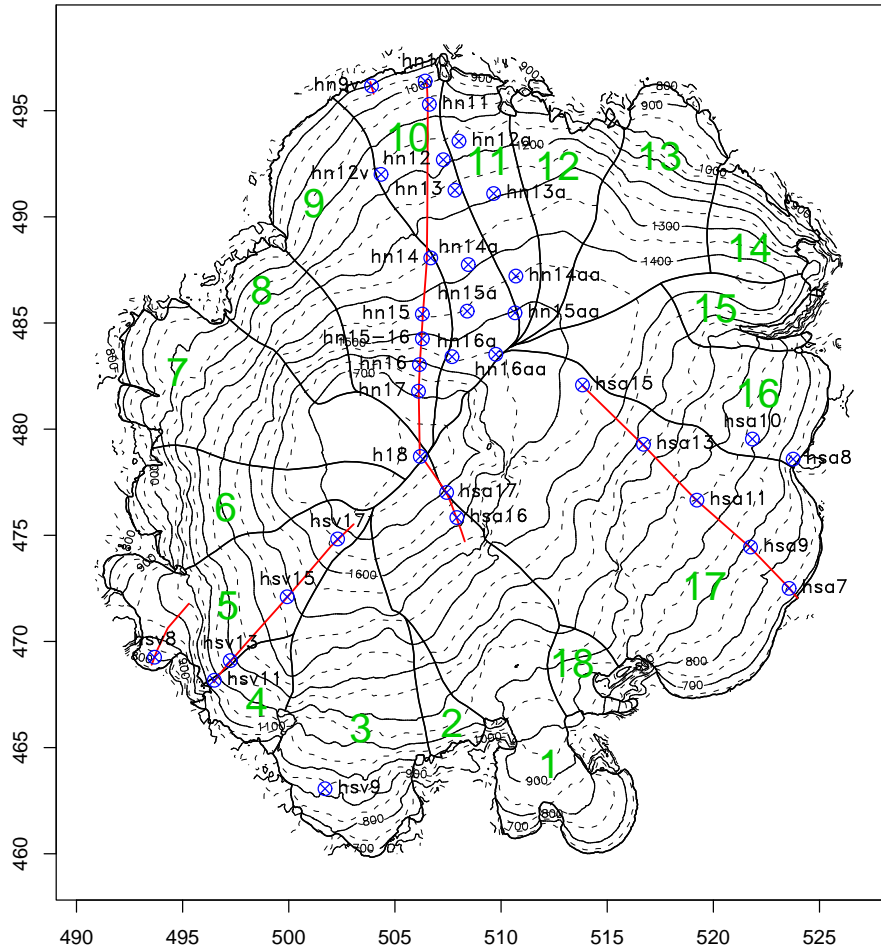


Figure 1: Map of the Hofsjökull ice cap showing ice flow basins and locations of mass balance stakes. Interpreted mass balance values are assumed to be located on red lines that are drawn down each of the monitored outlet glaciers. Ice flow basins are identified with sequential numbers between 1 and 18. Sátujökull is basins no. 10 and 11, Þjorsárjökull is basins no. 16 and 17 and Blágnjúpjökull is basin no. 5. Basin no. 9 is, in general, also taken to be a part of Sátujökull, but basins no. 10 and 11 are only considered in the interpretation of the mass balance measurements from Sátujökull at the National Energy Authority, since no stakes are located in the lower part of basin no. 9. The names and the areas of the ice flow basins are listed in Table 3.

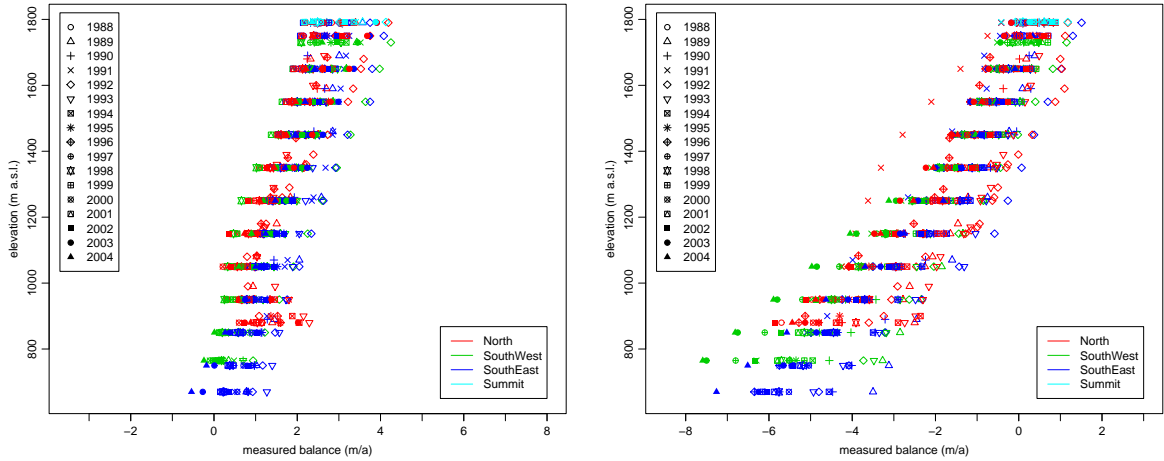


Figure 2: Observed winter (left) and summer (right) mass balance for three outlet glaciers from the Hofsjökull ice cap. Sátujökull is on the north side of the ice cap, Þjorsárjökull is on the southeast side and Blágnípujökull faces southwest.

The mass balance data have been reformatted and error checked as a part of the CWE and CE projects and are stored in a common format, which is used for mass balance data from several glaciers and ice caps that have been analysed in these projects (Jóhannesson, 2003).

Figure 2 shows the interpreted winter and summer mass balance as a function of elevation on each outlet glacier. The winter balance ranges from about  $-0.5 \text{ m}_{\text{w.e.}} \text{ a}^{-1}$  at the lowest elevations to about  $4 \text{ m}_{\text{w.e.}} \text{ a}^{-1}$  near the summit, and the summer balance ranges from about  $-7.5 \text{ m}_{\text{w.e.}} \text{ a}^{-1}$  at the lowest elevations on Þjorsárjökull and Blágnípujökull in the warmest years to about  $+1.5 \text{ m}_{\text{w.e.}} \text{ a}^{-1}$  near the summit in some years. The interannual variations in the winter balance at the same elevation on the same outlet glacier are about  $\pm 1 \text{ m}_{\text{w.e.}} \text{ a}^{-1}$ , comparatively independent of elevation. In the accumulation area, the interannual variations in the summer balance at the same elevation on the same outlet glacier are similar as for the winter balance. The range of the interannual summer balance variations widens downglacier and reaches about  $\pm 2 \text{ m}_{\text{w.e.}} \text{ a}^{-1}$  at the lowest elevations. The summer balance in the accumulation area of Sátujökull in 1991 (clearly visible as outliers in the upper left part of the summer balance panel of Fig. 2) is an exception from this pattern. This is due to tephra from an eruption in Hekla in January 1991, which affected the ablation of snow on the north side of the ice cap during this summer. The winter balance observed at the lowest elevations of Sátujökull deviates from the trend with elevation defined by other winter balance measurements from this glacier (outliers to the right at about 900 m a.s.l. in the winter balance panel of Fig. 2). This is due to snow drift into the lowest elevations near the terminus of Sátujökull, which affects a comparatively small area because the glacier is much steeper near the terminus than at other elevations.

### 3 The map of the ice cap

The surface of the Hofsjökull ice cap was mapped in 1983 using precision barometric measurements (Björnsson, 1988). The ablation area and the lowest part of the accumulation area below about 1200–1400 m a.s.l. was remapped by the Loftmyndir ehf. based on aerial photographs taken in August 1999 from an altitude of 8000 m. The summit area of the ice cap above 1600–1700 m a.s.l. was mapped by GPS instruments in August 2001 in connection with the drilling of a 100 m deep ice core near the summit (Þorsteinsson *et al.*, 2002).

The DTM used in the mass balance modeling described in this report is a composite, regular

100x100 m grid based on the aerial and GPS mapping from 1999 and 2001, respectively, where possible. The map from 1983 was used in the middle and lower parts of the accumulation area where the more recent measurements are not available. The glacier margin was, furthermore, digitised from the rectified aerial photographs from 1999, and ice flow divides were drawn manually to delineate the main ice flow basins. Figure 1 shows a contour map based on this new DTM together with the delineated ice flow basins and the margin of the ice cap. According to this mapping, the area of the ice cap in 1999 was 890 km<sup>2</sup>.

## 4 The MBT mass balance model

A new version of the MBT mass balance model for temperate glaciers (Jóhannesson *et al.*, 1993; Jóhannesson *et al.*, 1995b) was developed as part of the CWE and VVO projects. This model is a degree-day (temperature index) model that was developed for temperate glaciers in Iceland and the Nordic countries. Glacier accumulation and ablation are computed from daily temperature and precipitation observations at nearby meteorological stations. Daily melting,  $m$ , is computed according to the equation

$$m = DDF \max(T(z), 0) , \quad (1)$$

where  $T(z)$  is daily mean temperature at altitude  $z$  on the glacier, and  $DDF$  is the degree-day factor, which has separate values  $DDF_s$  and  $DDF_i$  for snow and ice, respectively.

The mass balance model may also be based on monthly mean temperatures,  $T_m$ , in which case fluctuations of the daily mean temperatures about the monthly average are assumed to be normally distributed with a standard deviation  $\sigma$  so that the sum of positive degree-days within the month,  $PDD$ , is given by

$$PDD = \frac{365/12}{\sigma\sqrt{2\pi}} \int_0^\infty T e^{-(T-T_m)^2/(2\sigma^2)} dT , \quad (2)$$

and the amount of melting is given by equation (1) with  $\max(T(z), 0)$  replaced by  $PDD$  (Braithwaite, 1985; Reeh, 1991; Jóhannesson *et al.*, 1995b).

When the snow thickness becomes less than a specified threshold, the degree-day factor is found as a weighted average of the degree-day factors for snow and ice. The reason for this is that the snow-line is not a sharp well-defined line at a certain altitude. Rather, it represents a transition from a surface of clean ice to a surface completely covered with snow, where patches of clean ice and snow will be mixed.

It is assumed that a part of the melting,  $r$ , is refrozen or stored as liquid water in the snow pack. The refrozen or retained water can be up to a given fraction of the snow remaining since the start of the current mass balance year. This leads to a delay in the onset of runoff from the annual snow pack with respect to the start of melting on the glacier. The ablation,  $a$ , is defined as the negative of the melting plus the refrozen or retained liquid water.

Temperature on the glacier is found using a constant vertical temperature gradient with altitude  $\Gamma$  (the so-called lapse rate is then  $-\Gamma$ )

$$T(z) = T_{stn} + \Gamma(z - z_{stn}) , \quad (3)$$

where the subscript *stn* denotes values at the meteorological station.

Precipitation,  $p$ , is computed using horizontal precipitation gradients,  $g_x$  and  $g_y$ , in addition to a vertical gradient,  $g_z$ ,

$$p = (1 + g_z(z - z_0))(1 + g_x(x - x_0) + g_y(y - y_0))p_c , \quad (4)$$

where  $x$  and  $y$  are horizontal coordinates, and  $p_c$  is corrected and scaled precipitation. The station precipitation is corrected for gauge losses using separate correction factors for snow and rain and

scaled with a constant correction factor in order to transfer it to a reference altitude  $z_0$  at location  $x_0, y_0$ .

Accumulation,  $c$ , is found by assuming a constant snow/rain threshold  $T_{s/r}$

$$c = p \text{ if } T(z) \leq T_{s/r}, \quad c = 0 \text{ if } T(z) > T_{s/r}. \quad (5)$$

The mass balance,  $b$ , is then given as the sum of the accumulation and the ablation

$$b = c + a = c - m + r. \quad (6)$$

The above expressions may be used to compute the cumulative mass balance over the winter and summer seasons by summing over the appropriate time periods.

On-line documentation (man-pages) describing the new model version in more detail are reproduced in the Appendix. The new version provides the possibility to specify a variation of the precipitation in the two horizontal dimensions in addition to a vertical precipitation gradient as described above. It may also be used to back-calculate precipitation at the mass balance stakes or at the assumed locations for the interpreted mass balance values from the observed mass balance over the winter and summer seasons. This feature of the model is being used to derive a data set of precipitation on the ice caps in the Icelandic highland, which is useful for verifying climate model simulations and statistical and physical models of precipitation in Iceland. New routines to couple the model to dynamic ice flow models and to specify a time dependent warming with a sinusoidal seasonal variation were also written.

## 5 Calibration of the mass balance model

The mass balance model is based on daily temperature and precipitation observations from the meteorological station at Hveravellir to the west of the ice cap (station no. 892, located at  $64^\circ 52'N$ ,  $19^\circ 34'W$ , 641 m a.s.l., data obtained from the Icelandic Meteorological Office), and calibrated against the winter and summer mass balance measurements from 1988–2004 that are described in Section 2.

Usually, stakes on the same outlet glacier are visited on the same day in the spring and autumn of each year or within a few day period. Occasionally, stakes on the same outlet glacier have, however, been visited with a time difference of up to a month or more. In order to take this into account, separate measurement days are used for all stakes and all years in the calibration of the mass balance model, without fixed assumptions about the beginning or end of the winter and summer seasons. In model simulations with the calibrated model, annual mass balance is computed by summing daily or monthly values over a whole mass balance year, which is assumed to start on 1 October.

The MBT model parameters are described briefly in the previous section, and in detail in the Appendix. Each parameter is denoted with a unique three letter abbreviation, *e.g.* “ddi” for the degree coefficient for ice,  $DDF_i$ . Some of them, but not all, are also denoted by a symbol such as “ $DDF_i$ ”. The model parameters that are fixed beforehand and are not varied in the calibration are given in Table 1. The fixed parameters are mainly of topographic nature, such as the altitude of the meteorological station, or describe meteorological characteristics, which are taken from other sources. The temperature lapse rate,  $-\Gamma$ , is based on values tabulated by Eypórssón and Sigtryggsson (1971) and also given by Einarsson (1976). The rain- and snow-correction factors are estimated by Sigurðsson (1990) for the meteorological station at Hveravellir. The temperature standard deviation,  $\sigma$ , is only used in modeling based on monthly temperature and precipitation data and is not relevant when daily data are used. The snow thickness threshold  $s_{is}$  is used to determine when the degree-day factor should found as a weighted average of the degree-day factors for snow (dds) and ice (ddi).

The reference location for the horizontal precipitation gradient,  $x_0, y_0$ , is chosen near the centre of the ice cap. It may be chosen arbitrarily because changes in the reference location can be exactly

Table 1: *Fixed model parameters.*

Parameter	Name	Value	Unit
Temperature lapse rate ( $-\Gamma$ )	grt	0.6	$^{\circ}\text{C}$ per 100 m
Snow/rain threshold ( $T_{s/r}$ )	tsn	1.0	$^{\circ}\text{C}$
Temperature standard deviation ( $\sigma$ )	sgm	3.0	$^{\circ}\text{C}$
Snow thickness used in degree-day computations	sis	0.3	$\text{m}_{\text{w.e.}}$
Refreezing ratio	rfr	0.032	1
Rain-correction factor	rko	1.32	1
Snow-correction factor	sko	2.0	1
Elevation of temperature station	elt	641	m a.s.l.
Elevation of precipitation station	elp	641	m a.s.l.
Reference $x$ -location for horizontal precipitation gradient ( $x_0$ )	xc0	510	km
Reference $y$ -location for horizontal precipitation gradient ( $y_0$ )	yc0	480	km
Starting elevation for vertical precipitation gradient ( $z_0$ )	elq	880	m a.s.l.

compensated by changes in the precipitation-correction factor,  $\text{pko}$ , but it is convenient to use a location near the centre of the area under consideration as is done here. The starting elevation,  $z_0$ , for the vertical precipitation gradient is chosen near the lower end of the elevation range of the ice cap. This parameter can also be chosen somewhat arbitrarily, because changes in the starting elevation may be nearly compensated by changes in other precipitation model parameters. However, it may be convenient to use a starting elevation within or close to the elevation range of the glacier, especially if the meteorological station is far outside this range.

The refreezing ratio  $\text{rfr} = 0.032$  given in Table 1 is different from the value  $\text{rfr} = 0.07$ , which was used by Jóhannesson *et al.* (1995b) and Jóhannesson (1997). The previous value was chosen based on measurements of the liquid water content of snow, and published values of similar parameters that have been used in hydrological modeling with the HBV model in Sweden and Norway (Jóhannesson *et al.*, 1993). This value was reconsidered on the basis of the much more extensive mass balance data from Hofsjökull used here compared with the data sets that were available in the previous modeling. This analysis indicates that the previous value of  $\text{rfr}$  is somewhat too high and a new value was chosen based on a similar optimisation as described below for the other optimised model parameters. The value of  $\text{rfr}$  is constrained by the retention capacity of snow and the temperature of the snow pack in the spring before melting starts on the glacier. Both the previous and the new optimised value are reasonable in this context. The refreezing ratio was not considered in the same detail as the other optimised model parameters because it has only a small effect on the modeled mass balance and its exact value is somewhat uncertain due to this reason. It is, therefore, grouped here together with other parameters with fixed values although its value is not the same as used in previous studies with the MBT model.

The remaining 6 model parameters were determined using non-linear least squares parameter fitting, minimising the total residual sum of squares (RSS) of the winter and summer mass balance measurements. This was done by computing the differences between measured and modeled winter and summer mass balance for all years at each location as an array, which was expressed as a function of the model parameters to be calibrated (mainly precipitation parameters and the degree-day coefficients for ice and snow). The non-linear least squares optimisation routine NLS from the statistical

Table 2: *Model parameters that were optimised in the calibration.*

Parameter	Name	Value	$\sigma_p$	Unit
Degree-day factor for ice ( $DDF_i$ )	ddi	7.44	0.07	mm <sub>w.e.</sub> °C <sup>-1</sup> d <sup>-1</sup>
Degree-day factor for snow ( $DDF_s$ )	dds	4.98	0.07	mm <sub>w.e.</sub> °C <sup>-1</sup> d <sup>-1</sup>
Precipitation-correction factor	pko	1.119	0.03	1
Precipitation/elevation gradient ( $g_z$ )	grp	0.207	0.01	1 per 100 m
Horizontal precipitation gradient in east direction ( $g_x$ )	pgx	0.0208	0.0014	1 per km
Horizontal precipitation gradient in north direction ( $g_y$ )	pgy	-0.0163	0.0013	1 per km

software package R (see “<http://www.r-project.org/>”) was used for finding the parameter values that minimised the sum of squares of the residuals. Mass balance measurements from the mass balance year 1990/1991 were not used in the calibration because of the effect of the eruption in Hekla in January 1991, which was mentioned in Section 2 about the mass balance data set. Also, measurements from the two lowest locations on Sátujökull were omitted because the observations there are affected by snow drift in a comparatively small area, as also mentioned in the section about the data set. The calibrated parameter values determined from all the mass balance data with these two exceptions (a total of 16 mass balance years) are given in Table 2. In addition to the optimised parameter values, the table also gives the statistical uncertainty of the parameter calibration corresponding to the residual variance,  $\sigma_{\delta b}^2$ , as given by

$$\sigma_p^2 = \text{tr}((A^T A)^{-1} \sigma_{\delta b}^2), \quad (7)$$

where the  $i$ -th component of the array  $\sigma_p^2$  is the variance of the  $i$ -th model parameter,  $\sigma_{\delta b}^2$  is the variance of the mass balance residuals,  $A$  is the Jacobian of the non-linear least squares equations, and  $\text{tr}$  denotes the diagonal elements of a matrix. The statistical uncertainty of the parameter estimates, as determined from equation (7) and tabulated in Table 2, may underestimate the actual uncertainty because of systematic variations in the mass balance residuals as is further analysed in Section 7 about the stability of the model calibration.

Figure 3 shows a comparison between the modeled and measured winter and summer mass balance. The model explains more than 80% of the variance in the winter balance data and over 95% of the variance in the summer balance data, leaving  $\sigma_{\delta b_w} = 0.40 \text{ m}_{\text{w.e.}} \text{ a}^{-1}$  and  $\sigma_{\delta b_s} = 0.42 \text{ m}_{\text{w.e.}} \text{ a}^{-1}$  as the RMS error (square root of the residual variance) for the winter and summer balance, respectively. The RMS errors of the winter and summer balance are similar in magnitude so that the larger proportion of the explained variance of the summer balance by the model is due to much larger year by year variations in the summer balance compared with the winter balance (*cf.* Fig. 2). Some of the largest deviations in Figure 3 are related to snow accumulation by snow drift into the lowest elevations near the terminus of the Sátujökull outlet glacier (the highest points near the lower end on the winter balance plot), which affects a comparatively small area, and an unusually high melting of snow due to tephra from the 1991 Hekla eruption that was deposited over large areas on Hofsjökull (relatively low points to the right on the summer balance plot). The corresponding data points from 1990/1991 and the lowest elevations on Sátujökull were not used in the calibration and they are not used in the computation of the explained variance or the RMS values reported above, but these data are shown in Figures 2 and 3 for completeness.

Figures 4 and 5 show the simulated average specific net mass balance and annual precipitation for 1981–2000 on Hofsjökull based on monthly temperature and precipitation observations for Hveravellir during the same period. The simulated mass balance distribution agrees well with the overall spatial

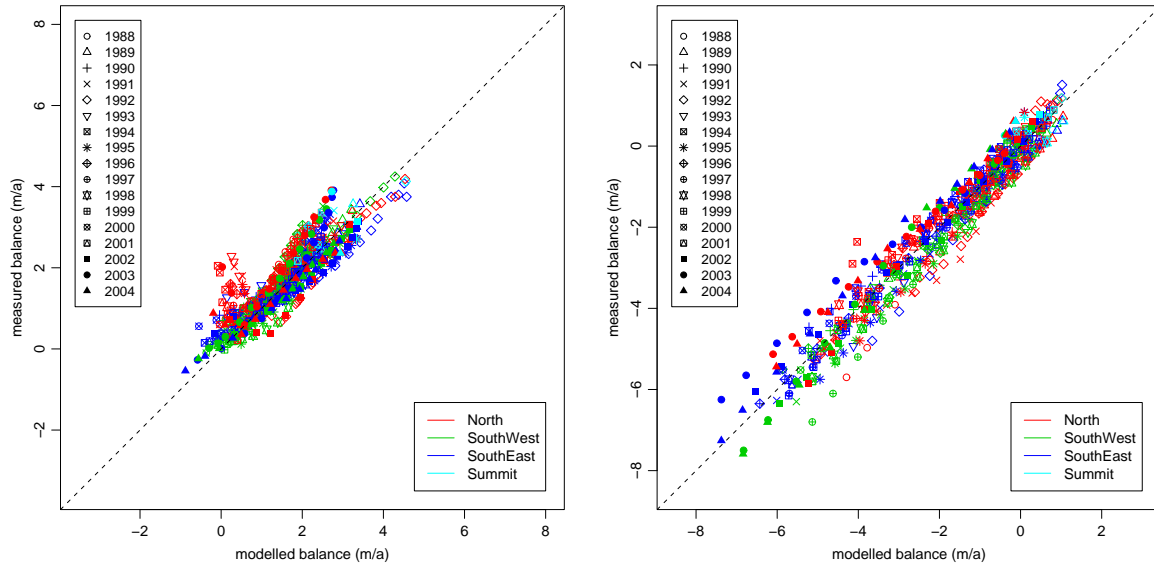


Figure 3: *Scatterplots of the modeled and measured winter (left) and summer (right) mass balance 1988–2004 including the mass balance year 1990/1991 and the observations from the lowest elevations on Sátuþjökull, which were not used in the model calibration.*

distribution of the mass balance data, with an ELA below 1200 m a.s.l. on the southern and southeastern flanks of the ice cap rising to about 1300 m on the western and northwestern sides. A simulation of the average mass balance during the same period based on daily temperature and precipitation from Hveravellir gives almost identical results (within  $0.15 \text{ m}_{\text{w.e.}} \text{ a}^{-1}$ ) to the results obtained with monthly values.

The simulated specific net balance averaged over the ice cap for the period 1981–2000 is close to zero within  $0.1 \text{ m}_{\text{w.e.}} \text{ a}^{-1}$ , which agrees well with the observation that the ice cap does not seem to have been far out of equilibrium during these decades. The average precipitation during the same period reaches a maximum of  $3.8 \text{ m a}^{-1}$  in the southern and southeastern part of the summit area, and the average precipitation for the whole ice cap for this period is  $2.4 \text{ m a}^{-1}$ . Due to the northwest to southeast precipitation gradient, the simulated, average precipitation in the southeastern ice flow basins (basins 1 and 15–18 in Fig. 1) is about  $2.6 \text{ m a}^{-1}$ , whereas it is about  $2.0 \text{ m a}^{-1}$  in the northwestern ice flow basins (basins 7–11 in Fig. 1).

## 6 Average mass balance of ice flow basins

Computing the specific net balance of individual ice flow basins (*cf.* Fig. 1) is a powerful test of the realism of the simulated mass balance distribution. As mentioned above, there are indications that the ice cap has been comparatively close to equilibrium in the period 1981–2000. This does not only apply to the whole ice cap, but also to the main ice flow basins, which seem to have been close to equilibrium individually during this period (the main exception being surges in parts of Þjórsárjökull in 1992 and 1994). A strong disequilibrium over an entire ice flow basin for many years may be expected to lead to an advance or retreat of the corresponding part of the ice margin. Thus, widely different values of the average net balance between the main ice flow basins over a period as long as 20 years may be expected to lead to similarly different patterns in the variations of the ice margin on different sides of the ice cap. One may, thus, assume that the geometry of the ice cap has adjusted to the long term average mass balance distribution so that the specific net balance of the individual ice flow basins over a sufficiently

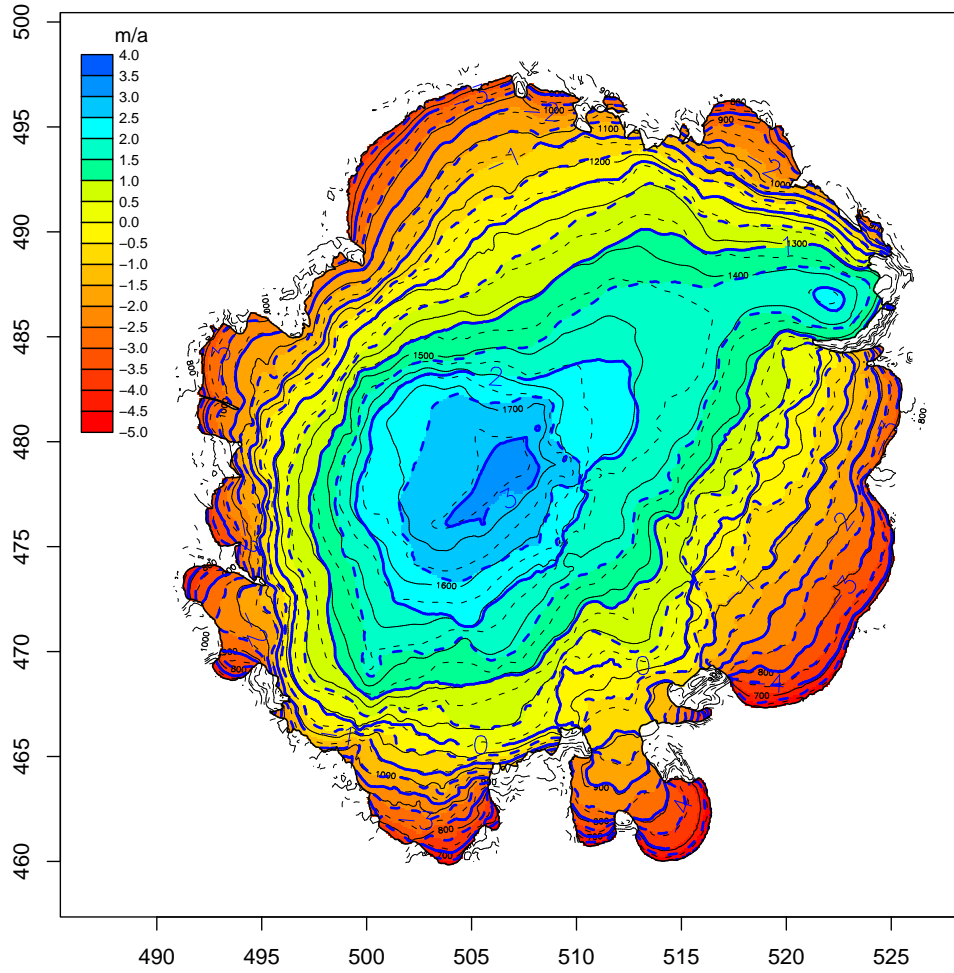


Figure 4: Simulated average specific net mass balance of the Hofsjökull ice cap for the period 1981–2000 in  $m_{w.e.} a^{-1}$  (color image and thick blue contours). Thin black contours show the elevation on the ice cap.



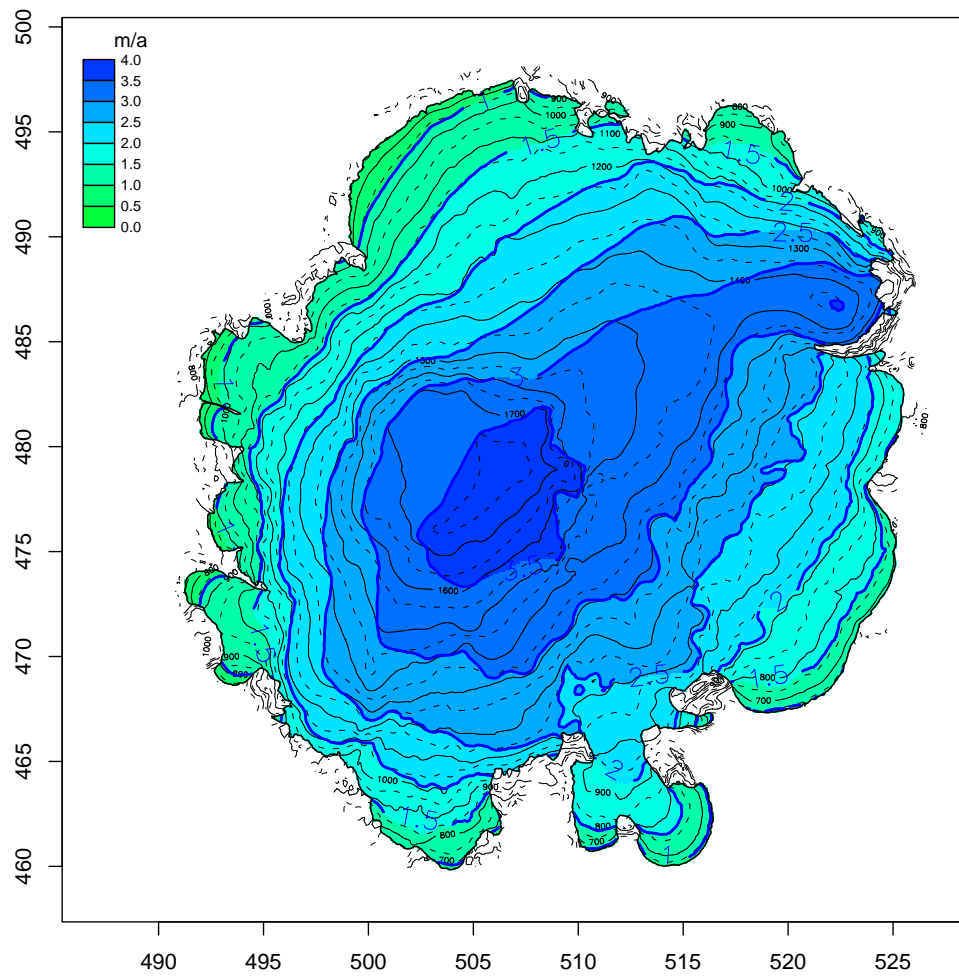


Figure 5: Simulated average annual precipitation on the Hofsjökull ice cap for the period 1981–2000 in  $\text{m a}^{-1}$  (color image and thick blue contours). Thin black contours show the elevation on the ice cap.

Table 3: Simulated average specific net mass balance for ice flow basins on the Hofsjökull ice cap for the period 1981–2000. Figure 1 shows the division of the ice cap into ice flow basins.

No.	Ice flow basin	Area (km <sup>2</sup> )	Net balance (m <sub>w.e.</sub> a <sup>-1</sup> )
1	Múlajökull	91	+0.12
2	Between Múlajökull and Blautukvísarjökull	9	+0.34
3	Blautukvísarjökull	73	−0.12
4	Between Blautukvísarjökull and Blágnípujökull	15	+0.02
5	Blágnípujökull	52	+0.06
6	Blöndujökull	39	+0.42
7	Kvísarjökull	66	+0.24
8	Between Kvísarjökull and Sátujökull	26	+0.07
9	Sátujökull, western part	72	−0.12
10	Sátujökull, central part	53	−0.04
11	Sátujökull, eastern part	29	−0.15
12	Between Sátujökull and Illviðrajökull	31	+0.30
13	Illviðrajökull	51	+0.10
14	Miklafell, northern part	19	+0.49
15	Miklafell, southern part	18	+1.15
16	Þjórásarjökull, northern part	56	+0.24
17	Þjórásarjökull, southern part	180	−0.07
18	Between Þjórásarjökull and Múlajökull	10	−0.70
—	Hofsjökull (whole ice cap)	890	0.07

long time period should be close to zero if the ice cap has been close to equilibrium during this period.

Table 3 shows the simulated average specific net balance over the 18 ice flow basins that are delineated in Figure 1. The last line of the table shows, as mentioned above, that the average net balance over the whole ice cap is close to zero. It should be noted in this connection, that the total mass balance over the whole ice cap in the period 1981–2000 is not considered in the model calibration at all. Therefore, the result that the average balance during this period is not far from zero is an independent verification that the mass balance model is not far off, although the average mass balance of the whole ice cap during this 20 year period is of course not well known. The absolute magnitude of the net balance in 14 of the 18 ice flow basins is less than  $0.3 \text{ m}_{\text{w.e.}} \text{ a}^{-1}$  and the mass balance in many of them has a magnitude of about  $0.1 \text{ m}_{\text{w.e.}} \text{ a}^{-1}$  or less. In addition, 3 of the 4 remaining basins, with mass balance greater than  $0.3 \text{ m}_{\text{w.e.}} \text{ a}^{-1}$  in magnitude, are smaller than about  $20 \text{ km}^2$  in area, so that small errors in the delineation of ice divides may lead to comparatively large errors in the specific balance there. The results tabulated in Table 3 provide an important verification of the main assumptions that underly the mass balance modeling, *i.e.* that the same degree-day coefficients for ice and snow may be used for the whole ice cap, and that the main features in the distribution of precipitation over the ice cap are captured by the horizontal and vertical precipitation gradients. Furthermore, these results support the extrapolation of observations, that are limited to only three of the many outlet glaciers, to the rest of the ice cap (*cf.* Fig. 1).

The simulated distribution of precipitation over the ice cap is of course based on very simple assumptions, which do not represent orographic processes in the generation of precipitation by air flow over mountains. In particular, the vertical precipitation gradient is somewhat unrealistically assumed to have the same effect at all locations at the same altitude, without any considerations about the up-

stream or downstream mountainsides corresponding to the daily or the most frequent wind directions. Although the analysis of the average specific mass balance within ice flow basins indicates that the main features in the simulated mass balance distribution are realistic, there is an interesting pattern in the modeled deviations from near zero mass balance. Two of the ice flow basins with a comparatively large positive deviation from near zero mass balance in Table 3 are areas no. 6 and 14 (Blöndujökull, and the northern part of Miklafell), where the modeled mass balance is about  $+0.5 \text{ m}_{\text{w.e.}} \text{ a}^{-1}$  in both cases. Ice flow basin no. 7 (Kvísíslajökull) also has a relatively large area with a positive mass balance of  $+0.24 \text{ m}_{\text{w.e.}} \text{ a}^{-1}$ . Those three basins are on the lee side of the ice cap in southeasterly winds, which are the main wind directions that carry wet air masses towards the ice cap. It is possible that the simple precipitation model simulates too much precipitation in these areas due to the fact that the effect of a precipitation shadow on the lee side of mountains is not properly taken into account. The largest positive mass balance in area no. 15 (southern part of Miklafell) cannot, however, be explained by this effect, nor can the negative mass balance in area no. 18, which of course is very small. The positive mass balance in areas 14–16 may indicate that the precipitation model simulates slightly too much precipitation near the northeastern margin of the ice cap. It is possible that some of these systematic deviations may be explained when a more realistic precipitation model, which is under development at IMO, will be applied in the next phase of mass balance modeling of Hofsjökull.

## 7 Stability of the model calibration

The stability of the obtained parameters was investigated by redoing the calibration with subsets of the data. The main calibration is based on data from 16 years, that is all data in the period 1988–2004, except for the mass balance year 1990/1991 and the lowest locations on Sátujökull. The calibration was carried out independently for the 8 first and 8 last years and for the 8 coldest and 8 warmest years from the set of 16 years used in the main calibration. The mean annual temperature at Hveravellir for the 8 warmest years was  $1.2^\circ\text{C}$  higher than for the 8 coldest years, which corresponds to the expected warming over 40–50 years according to typical scenarios for climate change in the North Atlantic area in the future (see later). The calibration was also carried out for the original raw stake data, which has not been interpreted to yield mass balance as a unique function of elevation on each side of the ice cap as described in Section 2 about the mass balance data set. Finally, the calibration was carried out separately for the three outlet glaciers. In that case, the horizontal precipitation gradients,  $g_x$  and  $g_y$ , were fixed at the values obtained in the main calibration because these parameters are not well constrained by data from only one outlet glacier. Table 4 shows that the calibrated parameter values are confined to comparatively narrow ranges and thus seem to be well constrained by the mass balance measurements.

The error in the parameter estimates may be computed from equation (7), which yields the statistical uncertainty of the parameters,  $\sigma_p$ , on the assumption that the mass balance residuals are statistically independent and all have the same variance  $\sigma_{\delta b}^2$ . Each parameter set from each calibration has its own set of  $\sigma_p$  values. These values are all similar for each parameter, except that the precipitation parameters  $p_{ko}$  and  $g_{rp}$  are not well constrained for Sátujökull. The table only gives typical values for  $\sigma_p$  corresponding to each parameter. The uncertainty of the precipitation parameters for Sátujökull is 2–5 times greater than the  $\sigma_p$  values given in the table. The mass balance residuals vary systematically between years and  $\sigma_p$  may underestimate the error in the parameter estimates substantially. A better measure of the uncertainty in the parameter estimates is given by the half range,  $\Delta p$ , which for each parameter is computed from the actual range of the estimated parameters for the different calibrations. The  $\Delta p$  values in Table 4 are determined as half the difference between the maximum and the minimum of the parameters corresponding to data sets that span the whole ice cap, *i.e.* the last three parameter sets corresponding to individual outlet glaciers are not considered.

The degree-day coefficients,  $ddi$  and  $dds$ , are both confined to comparatively narrow ranges within

Table 4: Model parameters estimated from subsets of the mass balance data. Names of the parameters and the corresponding symbols are given in Table 2. The two last lines give two different error estimates for the parameters (see text). The half range,  $\Delta p$ , is computed from the first 6 parameter sets only.

Data	ddi (mm <sub>w.e.</sub> °C <sup>-1</sup> d <sup>-1</sup> )	dds (mm <sub>w.e.</sub> °C <sup>-1</sup> d <sup>-1</sup> )	pko (1)	grp (1)	pgx (1 per km)	pgy (1 per km)
All 16 years	7.44	4.98	1.119	0.207	0.0208	-0.0163
First 8 years	7.26	5.68	1.141	0.194	0.0173	-0.0189
Last 8 years	7.61	4.52	1.155	0.201	0.0236	-0.0107
Coldest 8 years	7.45	5.50	1.118	0.193	0.0194	-0.0187
Warmest 8 years	7.53	4.70	1.192	0.202	0.0206	-0.0114
Stakes	6.82	5.12	1.095	0.225	0.0246	-0.0096
Sátujökull	6.63	5.14	0.731	0.414	—	—
Blágnípujökull	7.96	5.36	1.158	0.206	—	—
Þjórsárjökull	7.16	4.75	1.123	0.188	—	—
Typical $\sigma_p$	0.1	0.1	0.04	0.015	0.002	0.002
Half range $\Delta p$	0.4	0.6	0.05	0.02	0.004	0.0045

about 10% of the values from the main calibration. The precipitation parameters are more uncertain in a relative sense, but as they mostly specify terms that are added together to compute the modeled precipitation, the effect of this uncertainty on the modeled precipitation or mass balance is not greater relatively than for the degree-day coefficients. The model parameters derived for each of the outlet glaciers independently for the period 1988–2004 are also consistent with the parameters that are found for the whole ice cap. The derived model parameters for the period 1988–2004 are in good agreement with the parameters that were found previously for Sátujökull only, based on data from the much shorter period 1988–1992 (Jóhannesson *et al.*, 1995b), and for Blöndujökull/Kvísíljökull and Illviðrajökull for the same period (Jóhannesson *et al.*, 1997). The degree-day factors for ice and snow are for example all in the comparatively narrow ranges 5.0–8.0 mm<sub>w.e.</sub> °C<sup>-1</sup> d<sup>-1</sup> and 4.5–5.7 mm<sub>w.e.</sub> °C<sup>-1</sup> d<sup>-1</sup>, respectively, for all these previous cases and for all the calibrations in Table 4.

The RMS error (square root of the residual variance) corresponding to the main calibration is  $\sigma_{\delta b} = 0.41$  m<sub>w.e.</sub> a<sup>-1</sup> (winter and summer residuals combined). A fairly stringent test of the reliability of the modeling is to compute the model error for a test period with a parameter set derived from a separate calibration period, which does not include any data from the test period. This was done in a checkerboard manner for the first/last and cool/warm data sets used in Table 4. The model derived from the first 8 years of data was applied to the last 8 years and the model corresponding to the last 8 years was applied to the first 8 years of data. In this manner, residuals were obtained for all 16 years, but in both cases the models were only applied to data that had not been used in the corresponding calibration. The RMS error for this experiment with first/last years was  $\sigma_{\delta b} = 0.45$  m<sub>w.e.</sub> a<sup>-1</sup>. Similar computations for the data sets from the cool/warm years also yielded  $\sigma_{\delta b} = 0.45$  m<sub>w.e.</sub> a<sup>-1</sup>. This small difference between results with disjoint calibration/test periods compared with results for the whole period indicates that the parameters are reliable and not significantly affected by overfitting of measurement errors.

A special study of the distribution of snowfall over the highest part of the glacier was carried out as a part of the VVO project by measuring the thickness of the winter snow layer in May 2003 at 36 locations distributed over an area of about 40 km<sup>2</sup> near the summit of the ice cap (Þorsteinsson *et al.*,

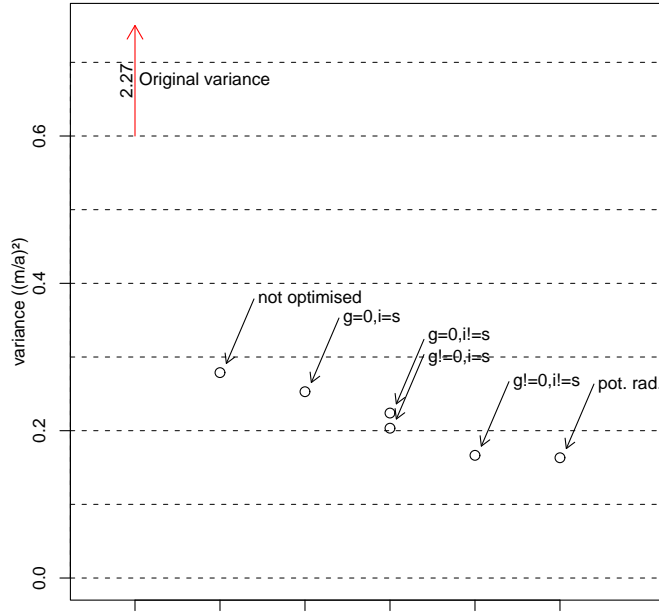


Figure 6: Residual variance of mass balance models with different specification of precipitation and melt parameters (see text for explanations). The level of detail of the models increases from left to right. The models denoted by “ $g=0, i!=s$ ” and “ $g!=0, i=s$ ” both introduce one additional feature compared with the model labeled “ $g=0, i=s$ ” and are therefore plotted at the same location on the x-axis. The original variance is computed from the deviations of the winter and summer mass balance from the average winter or summer balance, respectively, for the whole data set. All models are run for the same mass balance data from the period 1988–2004.

2003). The highest accumulation values were observed on the southern and southeastern part of the summit, with lower values found towards the northwestern part of the study area. These results are in general agreement with the simulated winter accumulation, but the northwest/southeast gradient in the simulated snow accumulation near the summit is not as steep as indicated by the measurements.

## 8 Comparison of different model types

The importance of the different components of the mass balance model was investigated by evaluating the performance of different model types with different specification of precipitation and melt parameters. Figure 6 shows the residual variance ordered according to increasing realism of the mass balance model. The original variance corresponds to the deviations of the winter and summer mass balance from the average winter or summer balance, respectively, for the whole data set (omitting the mass balance year 1990/1991 and the lowest locations on Sátujökull as before). All the models shown in the figure have a residual variance in the range 7–12% of the original residual variance. The first model on the left, labeled “not optimised”, which has the highest residual variance, is a mass balance model applied by de Woul *et al.* (2006), to the whole of Hofsjökull in a study of the importance of the firn layer for the hydrology of the ice cap. This model includes potential radiation in the formulation of a degree-day melt model (Hock, 1999), but is without horizontal precipitation gradients. It was calibrated manually, which explains to a large extent the comparatively poor performance compared with the automatically calibrated models. The next four models are different setups of the MBT model. The

model labeled “ $g=0, i=s$ ” is without horizontal precipitation gradients and the degree-day coefficients for ice and snow are assumed to be equal. This highly simplified model has a somewhat smaller residual variance than the model used by de Woul *et al.* The next two models add one additional aspect to the mass balance formulation each, the model labeled “ $g=0, i!=s$ ” has different degree-day coefficients for ice and snow, and the model labeled “ $g!=0, i=s$ ” has horizontal precipitation gradients. These models have 20–25% lower residual variance than the model used by de Woul *et al.* The model labeled “ $g!=0, i!=s$ ” is the MBT model corresponding to the main calibration, which is described in sections 5–7 and used to produce Figures 4 and 5. The model labeled “pot.rad”, which has a slightly lower residual variance than the MBT model corresponding to the main calibration, is the mass balance model of Hock (1999) with potential radiation, but with horizontal precipitation gradients included, and calibrated by the automatic calibration procedure, which was applied here for the MBT model (Thorsteinsson *et al.*, 2006).

As expected, the analysis shows that the use of different degree-day coefficients for ice and snow leads to a substantial improvement in the model. This is also obvious from the optimised values of  $dd_i$  and  $dd_s$  in Table 2, which are quite different from each other. The improved performance provided by a simple horizontal distribution of precipitation using linear gradients turns out to be even more important and leads to a larger reduction in the residual variance even when the degree-day coefficients for ice and snow are assumed to be equal. Using both different degree-day coefficients for ice and snow, and horizontal precipitation gradients, leads to a further decrease in the residual variance. A more complex degree-day melt model including potential radiation finally leads to a slightly lower residual variance by about 2% compared with the main calibration of the MBT model, but this step is much smaller than provided by the other incremental improvements. An important step in the reduction of the residual variance appears to be careful model calibration. The main calibration of the MBT model has 6 independent parameters and the model of Hock (1999) with horizontal precipitation gradients has 7 independent parameters that need to be determined. These parameters appear to be well constrained by the measurements, which contain 1106 observations of winter and summer balance, but the best combination of the parameters can be hard to find manually.

## 9 Back-calculation of precipitation at stake locations

One of the purposes of the mass balance modeling of Hofsjökull is to provide precipitation estimates for the development of a map of precipitation in the Icelandic highland, which is also a task under the umbrella of the CE/VO projects. Similar modeling for Langjökull and Vatnajökull is in progress for the same purpose. This precipitation data set comes from areas where there are few other precipitation measurements, but where precipitation estimates are important for many applications, such as the design and operation of hydroelectric power plants. These data may also have unique advantages for process studies of orographic precipitation because of the lack of other sources of precipitation estimates with a good spatial coverage from mountainous terrain. Precipitation estimates based on mass balance measurements in glaciated areas are also not affected by the undercatch of traditional precipitation gauges, and they may provide a dense spatial coverage with a limited measurement effort because the measurements are only carried out a few times a year. The results of this work will be reported in other reports and publications of the CE/VO projects, but here we will describe briefly how mass balance modeling was used to derive accumulated, seasonal precipitation estimates.

Raw mass balance measurements at stake locations or at the assumed locations of the interpreted mass balance data, are not suitable as precipitation estimates, because a part of the precipitation falls as rain, and because there is significant ablation even at the highest altitudes on the main Icelandic ice caps. However, the mass balance measurements, in particular the winter balance measurements, may provide very good estimates of accumulated precipitation if they are corrected for the proportion of the precipitation that fell as rain and for the ablation that occurred over the appropriate time period. In

most winters, there is little ablation in most of the accumulation area and most of the rain that falls is retained in the snow pack. Rain may, however, fall on the lowest part of the accumulation area and on most of the ablation area at any time of the year on the Icelandic ice caps, and ablation may also often be significant during the winter. It is, therefore, not suitable to assume that a certain subset of the uncorrected mass balance measurements, such as winter balance above a certain altitude, are useful as precipitation estimates.

The results of the mass balance simulations are affected by errors in both the simulated precipitation or snow accumulation, and also by errors in the simulated melting. Since the proportion of the precipitation corresponding to the snow accumulation is directly measured, it is possible to use this component directly, as it is measured in the field, and use the mass balance simulation only to estimate the melting and how much precipitation fell as rain. The MBT model can be run in a special mode to back-calculate precipitation in this manner, as mentioned in Section 4. This is implemented by fitting a separate precipitation correction for each stake and for each season so that the measured mass balance is exactly reproduced (see a more detailed description in the Appendix in the documentation of the  $-f$  model option). This procedure takes systematic errors in the precipitation model into account to a good approximation, especially if the ablation and rain are a small fraction of the precipitation, so that the model is only used to estimate a relatively small component of the total.

Errors in the simulated precipitation may be substantial in any individual year, although they are small as a long term average for a well calibrated model. In some areas of the ice cap, which are in a precipitation shadow (see discussion of this problem in Section 6), the precipitation model may also be systematically biased and it is important that such biases are not propagated into a precipitation data set that is used for further modeling or validation of other more elaborate precipitation models. The back-calculation procedure bypasses most of the flaws in the precipitation modeling in MBT, which is based on drastic simplifications using vertical and horizontal precipitation gradients.

Precipitation estimates obtained from glacier mass balance data are affected to some degree by snow drift. In most cases, stake locations have been chosen so that they are representative for large areas. Exposed ridges or depressions are, therefore, in general avoided as stake locations, but snow drift will, nevertheless, affect the observations to some degree. At a few locations, stakes are known to be severely affected by snow drift. Data from such locations have been omitted from the analysis as described in the previous sections. The mass balance data from most stake locations on Hofsjökull, which are used here, are believed to be representative for comparatively large areas on the ice cap and not substantially affected by snow drift. The error due to snow drift is, however, difficult to estimate quantitatively and it must be borne in mind when the back-calculated precipitation estimates are used.

Precipitation estimates obtained from glacier mass balance data are not directly comparable to traditional precipitation measurements at meteorological stations due to evaporation, in addition to problems due to snow drift and gauge losses, which were mentioned before. Traditional precipitation measurements are to some degree affected by evaporation from the gauges themselves from the time of precipitation to the emptying of the gauge. This effect is poorly known, but it has been estimated to be in range 2–7% of the measured precipitation on average for the type of gauges that are used in Iceland (Sigurðsson, 1990). The lower end of the range applies to stations with a high precipitation and the higher end of the range corresponds to comparatively dry stations. Evaporation or condensation from the surface of the glacier does, however, occur on every day of the year, whether it is wet or dry, whereas, the effect of evaporation on precipitation measurements from gauges only occurs on wet days (because the gauge is empty on dry days). Evaporation/condensation from the surface of glaciers in Iceland is not well known, but it has been estimated based on data from meteorological stations that were operated on Breiðamerkurjökull in S-Vatnajökull during the summer 1996 (Obleitner, 2000), and simulated by energy balance modeling (Sverrir Guðmundsson, personal communication 2006). These results indicate that evaporation dominates condensation for snow covered areas on average, whereas condensation is more important than evaporation from ice covered surfaces. The net result over the

summer for a meteorological station at 715 m a.s.l. near the equilibrium line on Breiðamerkurjökull in 1996 was about 20 mm of evaporation. Higher values in absolute magnitude may be expected at the lowest and highest altitudes on the glaciers. In general, one may, however, assume that total evaporation or condensation on the glaciers is much smaller in the annual average than the total precipitation, which tends to be larger on the glaciers than the average for the whole country.

In order to ensure that the simulated component of the precipitation is a sufficiently small part of the total, the model is only used to back-calculate precipitation when the corresponding seasonal mass balance is greater than zero, *i.e.* when the total melting is not greater than the total snowfall. This means that most winter balance measurements and some summer balance measurements from the highest altitudes in comparatively cold years may be used to provide back-calculated precipitation estimates. The interpreted mass balance data set for Hofsjökull from 1988–2004 contains a total of 1270 seasonal mass balance measurements, including the mass balance year 1990/1991 and the lowest locations on Sátujökull, which were omitted from the model calibration. Of those, 777 observations have been used to back-calculate precipitation, when the observations corresponding to negative mass balance values and the lowest locations on Sátujökull have been omitted. The mass balance from the year 1990/1991 was used to back-calculate precipitation as the tephra from the Hekla eruption did not affect the winter balance to a large degree, so that the data should be useful for this purpose.

## 10 The climate scenario

The climate change scenario of the CWE project, “The Climate, Water and Energy—Nordic climate scenario” (abbreviated CWE-NCS), is described by Rummukainen *et al.* (2003) and Räisänen (2003), and further GCM downscaling results for the Nordic countries are discussed by Räisänen *et al.* (2004). The scenario provides a projection of climate change in the Nordic countries for the period from 1990 to 2050 corresponding to the IPCC SRES B2 emission scenario (IPCC, 2001; Nakicenovic and Swart, 2000; Leggett *et al.*, 1992). The scenario is the average of scaled grids of mean monthly projections of four regional climate models over the North Atlantic and the neighbouring continental areas (the Swedish RCA-H and RCA-E models, and the Danish and Norwegian HIRHAM RCM models, see Rummukainen *et al.* (2003) for references describing these models). The RCM simulations use boundary conditions from global, transient climate change simulations by the ECHAM4/OPYC3 (Roeckner *et al.*, 1999) and HadCM2 (Johns *et al.*, 1997) coupled OAGCM models.

The four RCM simulations correspond to different time horizons and different scenarios of future anthropogenic forcing. Before averaging, the RCM model results were harmonised with respect to time horizon and emission scenario to correspond to the SRES B2 emission scenario by a scaling procedure described by Rummukainen *et al.* (2003) and Christensen *et al.* (2001). The domain of one of the RCM models (the Danish HIRHAM model) does not include Iceland. Therefore, the CWE-NCS scenario for Iceland used here is the average of the remaining three RCM simulations, rather than all four as for the Scandinavian continental area.

Figures 7 and 8 show the yearly mean temperature and relative precipitation change (%) specified by the composite CWE-NCS scenario. It is seen that the projected temperature change varies strongly over the North Atlantic Ocean so that Iceland is situated in a steep gradient in the warming between a local minimum south and east of Greenland to a maximum between northern Norway and Greenland. This relative minimum is a common feature of many, but not all, coupled global and regional climate model simulations in this area (IPCC, 2001, Räisänen *et al.*, 2004). It is possibly related to a projected weakening in the thermohaline circulation, which is associated with a reduced rate of deep water formation in the northern North Atlantic Ocean (*cf.* IPCC, 2001). A similar local minimum in the projected warming is seen in the raw output of the coupled OAGCM models.

For comparison, Figures 9 and 10 show the mean temperature change and the mean relative precipitation change computed from 5 OAGCM models forced with the B2 emission scenario (data



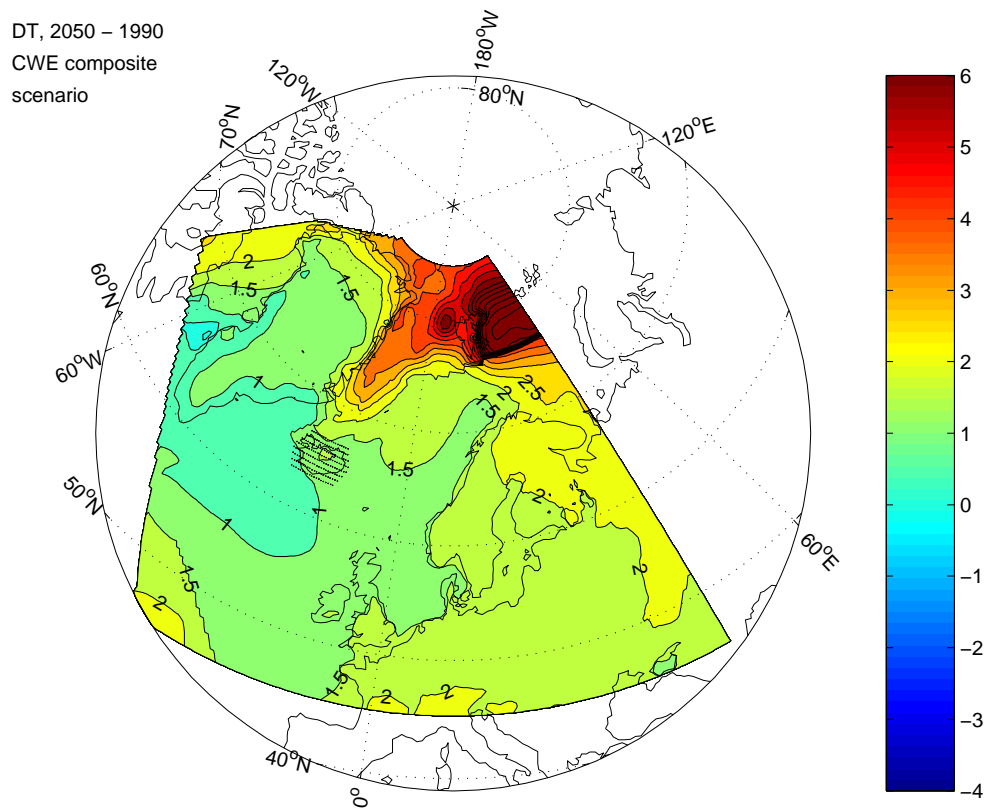


Figure 7: *The CWE-NCS temperature change scenario, 1990–2050. Symbols on and near Iceland show grid locations used to compute the average shown in Fig. 11.*

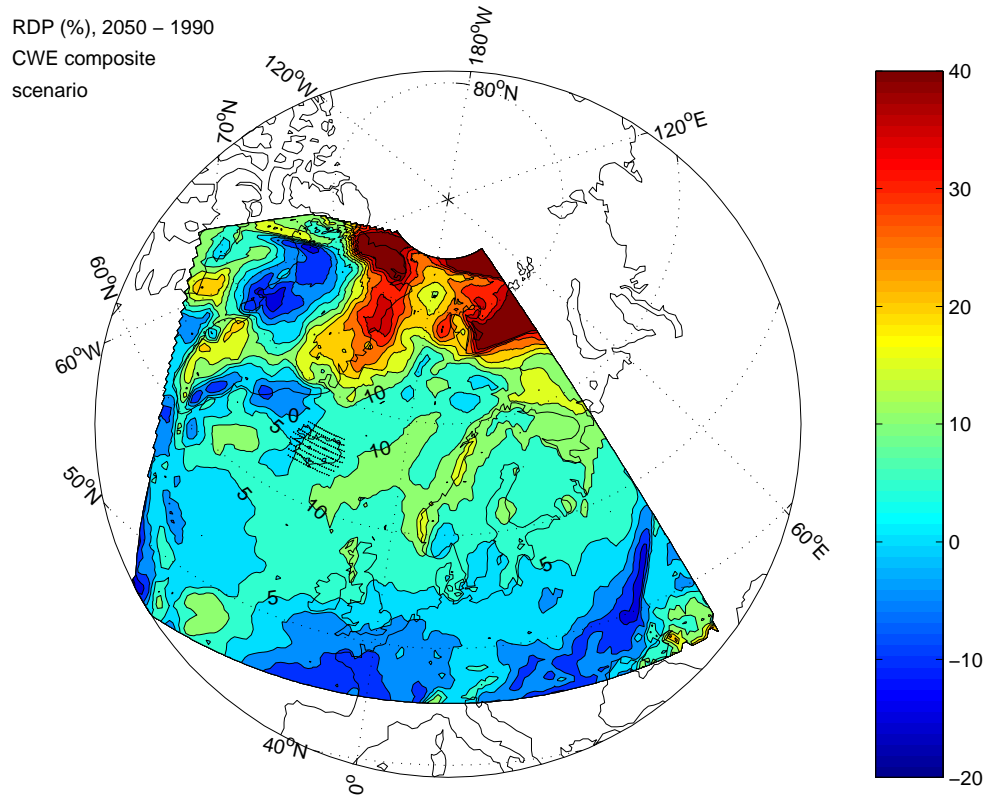


Figure 8: *The CWE-NCS relative precipitation change scenario (%), 1990–2050. Symbols on and near Iceland show grid locations used to compute the average shown in Fig. 11.*

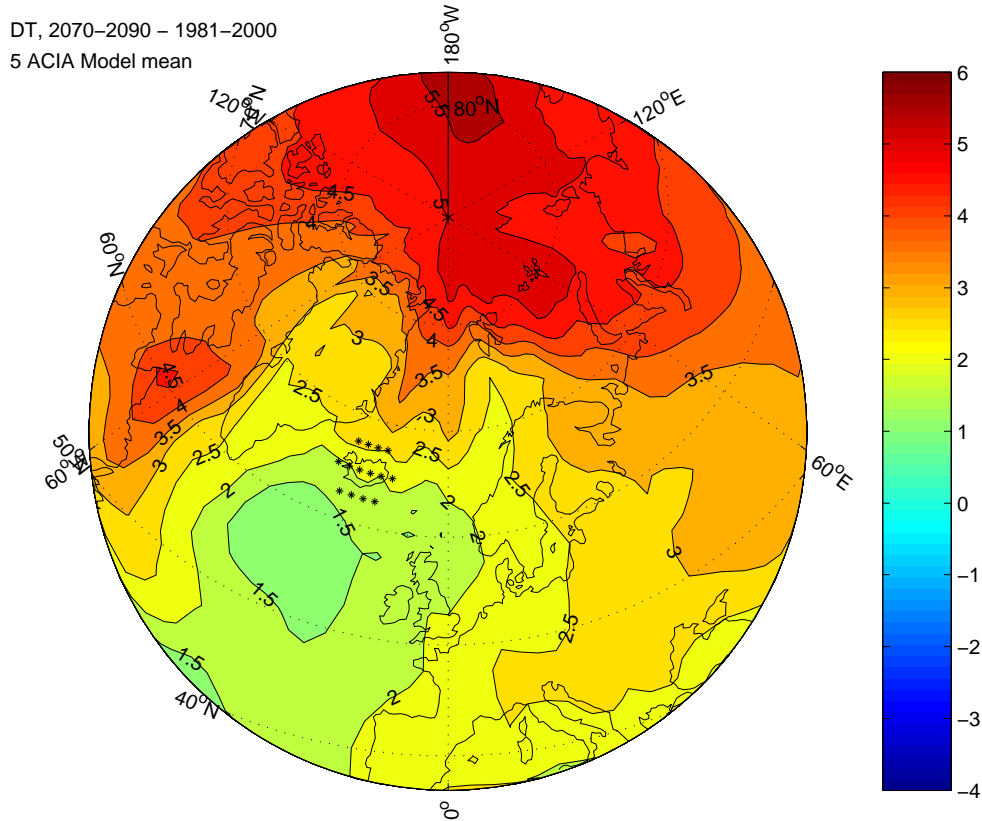


Figure 9: The five ACIA model average projected temperature change from 1981–2000 to 2071–2090. Symbols on and near Iceland show grid locations used to compute the average shown in Fig. 12.

obtained from the IPCC data distribution centre, “<http://ipcc-ddc.cru.uea.ac.uk>”; *GFDL*: Knutson *et al.*, 1999; *Had*: Gordon *et al.*, 2000; *Ech*: Roeckner *et al.*, 1999; *Ccc*: Flato *et al.*, 2001; *Csm*: Boville and Gent, 1998). These 5 models were used in the Arctic Climate Impact Assessment (ACIA, “<http://www.acia.uaf.edu>”).

There are many details that need to be considered when a scenario is applied to a particular location in hydrological or glaciological modeling. In spite of being long term averages over 8–20 year periods, the monthly data in Figures 7 and 8 contain statistical fluctuations and they need to be further averaged before they are applied in impact modeling (Rummukainen *et al.*, 2003; Räisänen, 2003). Figure 11 shows the projected seasonality of the temperature and precipitation change near Iceland as given by the average over the grid points shown in Figures 7 and 8. Similar results are obtained directly from raw OAGCM model output as seen in Figure 12, which shows the projected seasonality of the temperature and precipitation change for the 5 ACIA models (both the 5 model average and the individual models) near Iceland as given by the average over the grid points shown in Figures 9 and 10.

There are some fluctuations in the monthly CWE-NCS temperature signal averaged over Iceland, and especially in the precipitation signal (Figure 11), that appear to be caused by natural variability rather than being a climate change signal. This indicates that the monthly values averaged over the area near Iceland shown in Figure 11 are still too much influenced by natural variability to be used directly in impact analyses and need to be smoothed to extract a climate change signal suitable for use in the glacier modeling (*cf.* Rummukainen *et al.*, 2003).

In order to provide for more smoothing in the temperature change signal, the monthly values shown in Figure 11 were replaced by a least squares sinusoidal variation through the year. The minimum

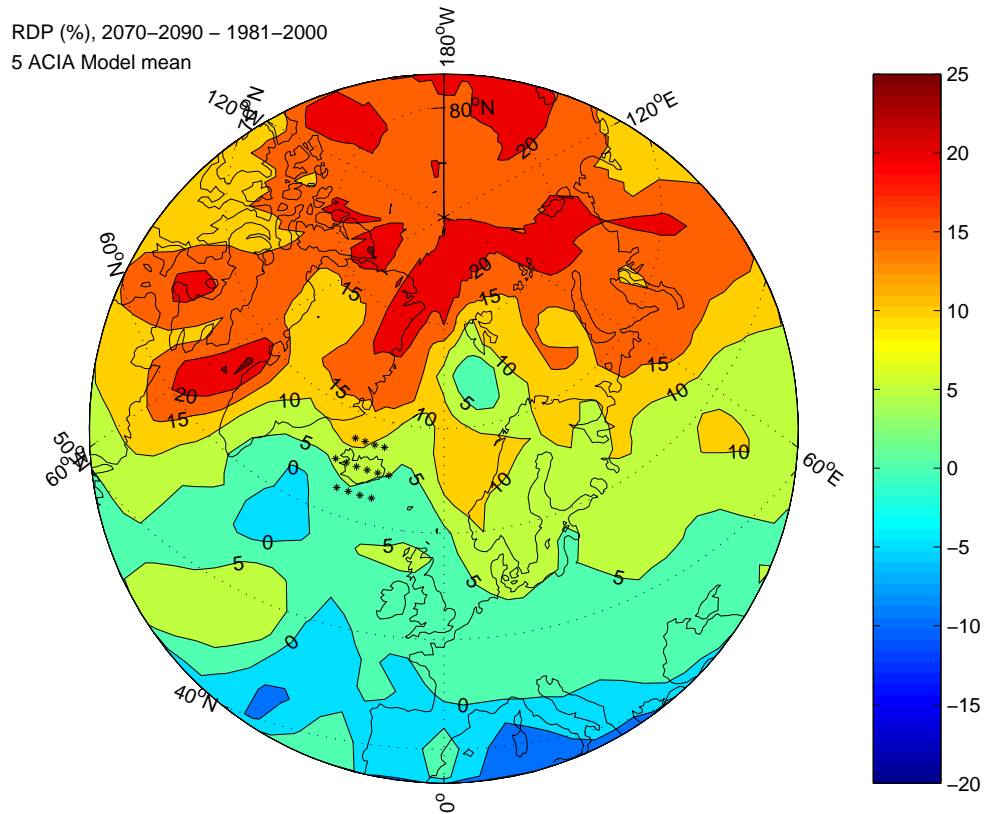


Figure 10: The five ACIA model average projected relative precipitation change (%) from 1981–2000 to 2071–2090. Symbols on and near Iceland show grid locations used to compute the average shown in Fig. 12.

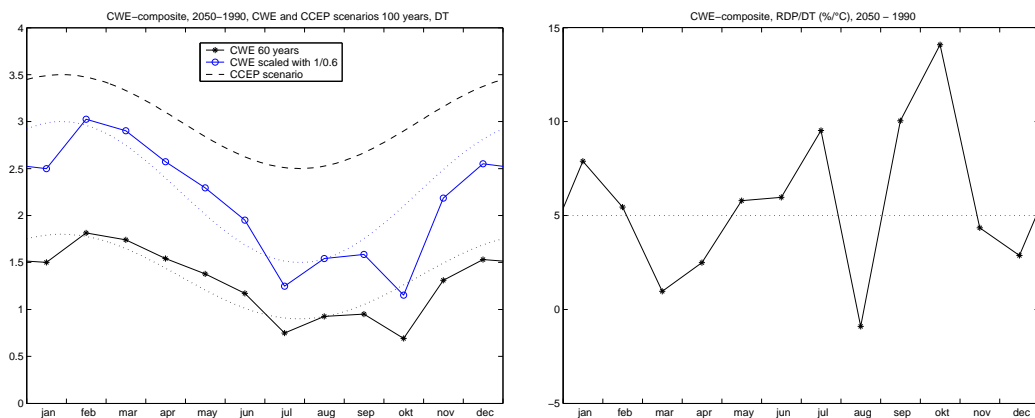


Figure 11: The monthly CWE-NCS temperature (left) and precipitation (right) change scenarios near Iceland (average over the area shown in Figs. 7 and 8), 1990–2050. The temperature figure also shows the 1990–2050 temperature change scaled by 1/0.6 which is intended to represent the temperature change from 1981–2000 to 2081–2100 corresponding to the CWE-NCS scenario. The precipitation figure shows the relative precipitation change divided by the change in temperature. Dotted curves show the CWE-NCS scenarios that were used in mass balance modeling of glaciers in Iceland. The dashed curve shows the older CCEP temperature scenario (over a period of 100 years).

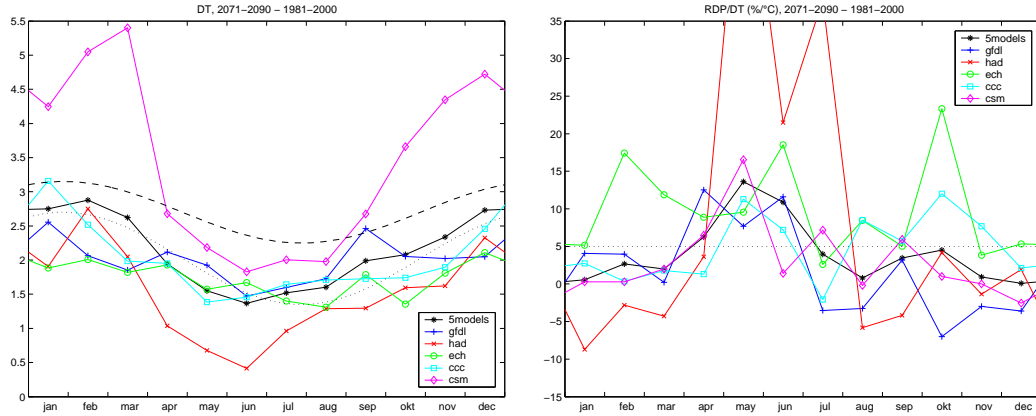


Figure 12: *The monthly average temperature (left) and precipitation (right) change near Iceland for the 5 ACIA OAGCM models (average over the area shown in Figs. 9 and 10), from 1981–2000 to 2071–2090. The precipitation figure shows the relative precipitation change divided by the change in temperature. Note that large relative changes in precipitation per degree of temperature change may result from low monthly temperature changes that may arise from statistical fluctuations caused by natural climate variability. This may partly be the reason for the high values of the Had curve during May and July. Dotted curves show the CWE-NCS scenarios that were used in mass balance modeling of glaciers in Iceland (changes over a time period of 90 years to be consistent with the model output). The dashed curve shows the older CCEP temperature scenario (also changes over 90 years).*

warming shown in Figure 11 occurs rather late in the summer, considerably later than for the 5 ACIA models shown in Figure 12. This appears to be caused by a comparatively low monthly value for the projected warming in October that is likely to be caused by a statistical fluctuation. Figure 13 shows the observed seasonal variation of temperature at the meteorological station at Hveravellir in the Icelandic highland in the period 1987–2003. It is seen that the temperature reaches a maximum in late July, about one month earlier than the minimum in the temperature signal in Figure 11. It appears likely that the seasonality of the temperature change will reduce the amplitude of the seasonal variation of the temperature within the year, rather than change its phase. Therefore, it was decided to use the phase of the observed seasonal temperature variation at Hveravellir in the temperature scenario rather than the phase of the simulated temperature variation shown in Figure 11. The temperature scenario thereby specifies a warming varying from a winter maximum of  $+0.3^{\circ}\text{C}$  per decade in late January and to a summer minimum of  $+0.15^{\circ}\text{C}$  per decade in late July with a sinusoidal variation between these values (dotted curve in Figure 11).

The monthly fluctuations in the CWE-NCS relative precipitation change in Figure 11 appear without a clear climate change signal and they are quite inconsistent between the different RCM models (*cf.* Figures 2 and 4 in Rummukainen *et al.*, 2003). The precipitation change was, therefore, simplified to a constant relative change of 5% per degree of warming independent of season.

The seasonal temperature and precipitation changes from the 5 ACIA OAGCM models near Iceland (*cf.* Fig. 12) show a large inter-model scatter, especially for the precipitation change. The 5 model mean temperature change shows a similar seasonal variation as the CWE-NCS temperature change (Fig. 11, left), except that the minimum warming appears early in the summer in most of the ACIA models but rather late in the summer according to the CWE-NCS composite scenario data. The seasonal variation in the 5 model mean relative precipitation change per degree of warming bears little resemblance to the corresponding CWE-NCS variation (Fig. 11, right). This supports the decision to use a constant relative precipitation change per degree of warming independent of the season in the mass balance modeling of glaciers in Iceland.

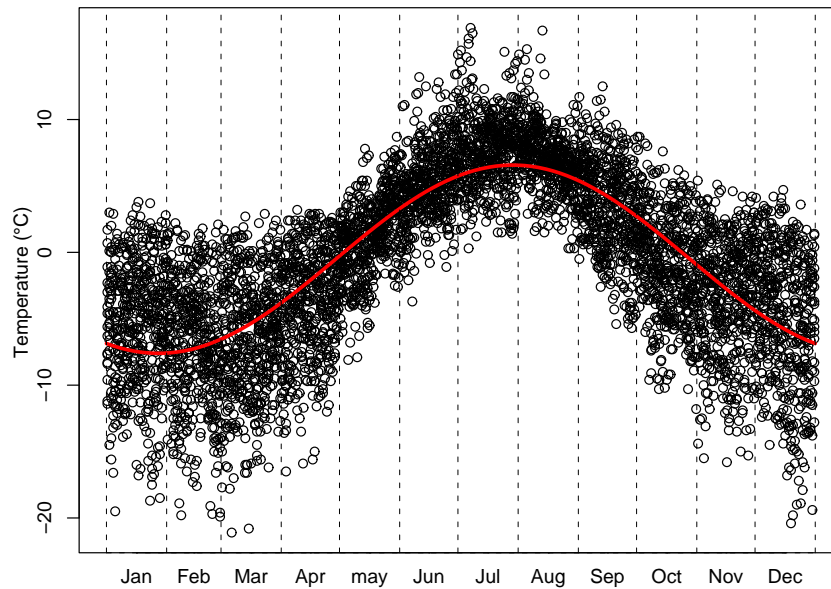


Figure 13: *Seasonal temperature variation at Hveravellir, 1987–2003.*

Finally, the question of baseline needs to be considered. The composite CWE-NCS scenario is intended to show change with respect to the year 1990. Here it is assumed that this means change with respect to an average climate of the period 1981–2000. Many glaciers in Iceland seem to have been roughly in equilibrium in the period 1981–2000, advancing a little during the early part of the period and retreating near the end of the period. This period is, thus, a convenient reference period for mass balance modeling studies because one would expect the average mass balance of many non-surging glaciers in this period to have been near zero.

The CWE-NCS climate scenario projects rather low temperature increase for Iceland, compared with neighbouring areas, especially during the summer. This is due to the local minimum in the warming in the North Atlantic Ocean that is simulated by some coupled OAGCMs as discussed above. The observed warming in Iceland in the last two to three decades has not been characterised by much lower warming during the summer compared with the winter as further described in the next section, in fact the summer warming is quite similar to the mean annual warming for the meteorological station at Hveravellir. It is the magnitude of the summer warming that is most important for changes in glacier mass balance due to climate changes, and to a lesser degree the spring and autumn warming. Therefore, it is important to consider the question of the seasonality of the temperature change in some detail. The possible future reduction in the strength of the thermohaline circulation in the North Atlantic Ocean projected by some coupled OAGCMs must be considered highly uncertain and this presents a major problem for hydrological and glaciological modeling of the consequences of climate warming in Iceland.

In view of these circumstances, the climate change scenario from the previous Nordic project, Climate Change and Energy Production (CCEP) (Sælthun *et al.*, 1998; Jóhannesson *et al.*, 1995a) was also used in the mass balance and dynamic modeling of Hofsjökull (the results of the dynamic modeling are described in Jóhannesson *et al.*, 2004). This scenario, which is shown as dashed curves in Figures 11 and 12, prescribes a yearly mean warming of  $0.3^{\circ}\text{C}$  per decade, varying from a winter maximum of  $+0.35^{\circ}\text{C}$  per decade to a summer minimum of  $+0.25^{\circ}\text{C}$  per decade, and a relative precipitation change of 5% per degree of warming independent of the season as in the CWE-NCS scenario. This warming is closer to the projected warming in other ocean areas on a similar latitude as Iceland, although not as high as in Scandinavia or other continental areas in this latitude range.

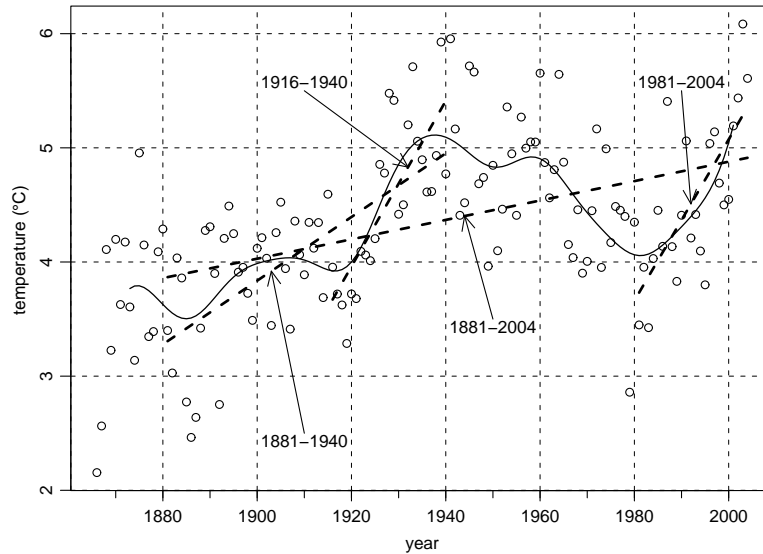


Figure 14: *Annual mean temperature in Reykjavík, 1866–2004. The thin solid curve shows an exponentially weighted running average with a 10 year time window. The dashed line segments show linear least squares fits to the annual data in the four time windows specified by the figure labels.*

The use of the climate change scenario from the previous CCEP study serves the purpose to investigate the consequences of climate changes in case the strength of the thermohaline circulation in the North Atlantic Ocean is not reduced as much as projected by some coupled OAGCMs. It also provides a direct comparison with the results of the previous study. Both these scenarios were employed with and without specifying the precipitation change, that is, the mass balance model was, in addition to the full scenario, also run for a case where only the temperature was changed and not the precipitation. This was done in order to investigate the relative importance of the temperature and precipitation changes, and also because local precipitation changes must be considered more uncertain than temperature changes as can be clearly seen from a comparison of Figures 7 and 8.

## 11 Observed temperature changes in Iceland

There is large uncertainty about the seasonality of future temperature changes in Iceland as discussed in the previous section. Measured changes in temperature in Reykjavík, southwestern Iceland, since 1866 and at the meteorological stations Hveravellir, in the central Icelandic highland, Nautabú, central northern Iceland, Kirkjubæjarklaustur, central southern Iceland, and Fagurhólsmyri, southeastern Iceland, since 1981, were analysed to shed some light on this question. Figure 14 shows annual mean temperature in Reykjavík between 1866 and 2004 (data from the Icelandic Meteorological Office). The figure shows a generally warming trend since the last two decades of the 19<sup>th</sup> century with the largest rate of warming in the two periods 1920–1940 and 1980–2004. The total warming in Reykjavík over the period since the 1880s is about 1°C, which is similar or somewhat larger than the observed global average warming of 0.4–0.8°C since the late 19<sup>th</sup> century (IPCC, 2001). The warming since the last two decades of the 19<sup>th</sup> century or the early 20<sup>th</sup> century at other Icelandic weather stations is similar as in Reykjavík. The warming in Iceland, thus, does not seem to be lower than the global average

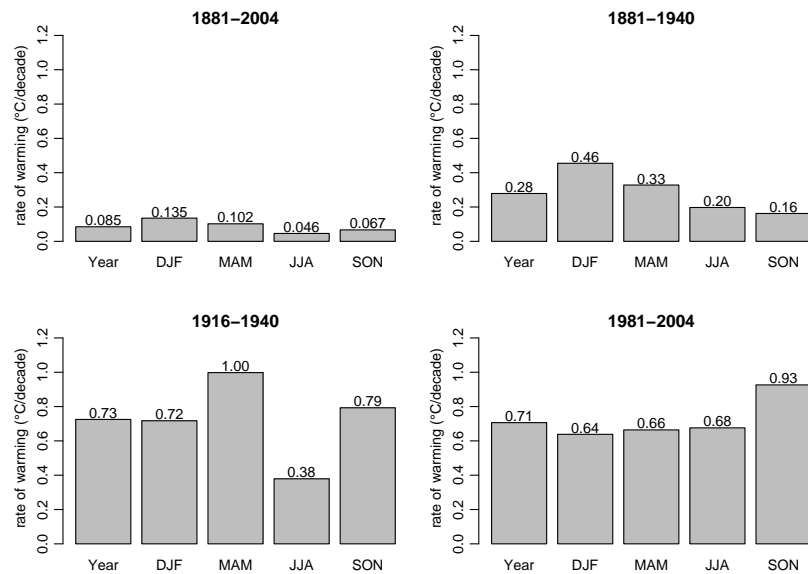


Figure 15: Average change per decade in the annual and seasonal mean temperature in Reykjavík for the four time periods that are shown as dashed line segments in Fig. 14. The rate of warming in each time period is determined as the slope of a linear least squares fit to the annual data.

according to these data.

Figure 15 shows the rate of warming per decade in Reykjavík for the annual mean temperature and for the seasonal mean temperature in DJF, MAM, JJA and SON within the four time windows 1881–2004, 1881–1940, 1916–1940 and 1981–2004 that are shown as dashed lines in Figure 14. The time windows were chosen so that, in addition to the entire period 1881–2004, and the shorter period 1881–1940, they cover the two main periods of rapid warming since 1881. The periods were defined so that they don't start or end at the most extreme years, such as 1919 or 1979, in order not to be too much affected by an *ad hoc* choice of the end points. Thus, the 25-year long period 1916–1940 starts in the cold years before the onset of the rapid warming of the 1920s and ends somewhat after the rate of warming started to decline. Similarly, the 24-year long period 1981–2004 starts near the coldest temperatures in the cool period 1975–1985, but after the extremely cold year 1979. The rates of warming shown by the bars in the lower two panels in Figure 15 should, therefore, reflect a “typical” rate of warming within these periods rather than a maximum rate of warming that can be achieved by artificial twisting of the beginning and end of the time windows.

The bar plots in Figure 15 show that the rate of rapid warming during the periods 1916–1940 and 1981–2004 is similar, that is about  $0.7^{\circ}\text{C}$  per decade in the annual mean. This is 5–10 times more rapid than the average rate of warming during the entire period 1881–2004. The seasonal variation of the warming is different in the different time windows. The two earlier periods starting in the late 19<sup>th</sup> century show the highest warming in winter and the lowest warming during the summer or fall seasons. The period 1916–1940 also has the lowest warming during summer, but the highest warming occurs during the spring and fall. The most recent period, 1981–2004, has the most rapid warming in the fall, but the rate of warming in the other seasons is similar.

Figure 16 shows the annual and seasonal rates of warming per decade for the period 1981–2004 for four weather stations from different regions in Iceland that have all been used for glacier mass balance modeling and Figure 17 shows the average of the annual and seasonal warming rates for all five weather



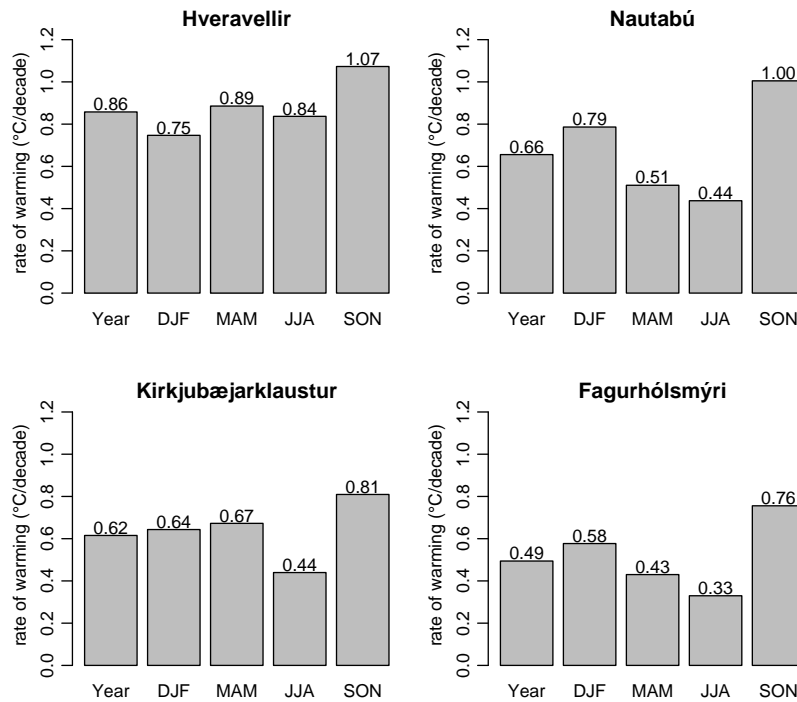


Figure 16: Average change per decade in the annual and seasonal mean temperature at four meteorological stations for the period 1981–2004.

stations during this period. The highest warming rate occurs in the fall at all five stations, but the lowest warming occurs in different seasons at the different stations. In Reykjavík, the warming is similar in the winter, spring and summer seasons. Nautabú, Kirkjubæjarklaustur and Fagurhólmseyri have the lowest warming in the summer, whereas Hveravellir has the lowest warming in the winter. Both the individual station data and the average of the five stations show a lower summer warming during 1981–2004 compared with the annual mean, although the difference is very small for Hveravellir. Thus, the seasonal variation of the warming is rather different in the different time windows and at the different stations shown in figures 15, 16 and 17, and it is not similar to the seasonality of the CWE-NCS scenario in the most recent time period. The summer warming at Hveravellir, which is close to Hofsjökull, is in fact quite similar to the annual mean warming.

According to the CWE-NCS climate scenario for Iceland, which is described in the previous section, the projected warming reaches a minimum during mid summer. The summer warming is only half of the maximum warming, which is assumed to take place during mid winter. This assumed seasonality implies the smallest possible effect on glacier ablation for a given value of the annual warming because the ablation is primarily sensitive to changes in temperature during late spring, summer and early fall. The assumed seasonality of the CWE-NCS scenario for Iceland is based on model results that seem to indicate the lowest rate of warming during late summer or fall (*cf.* Fig. 11), whereas observations of recent warming in Iceland show the most rapid warming in the fall season (*cf.* Figs. 16 and 17). Although it is not possible to draw firm conclusions regarding future climate warming in Iceland based on past trends in station data over a few decades, it seems worthwhile to consider additional scenarios with a less pronounced seasonality in addition to the CWE-NCS scenario. As described in the previous

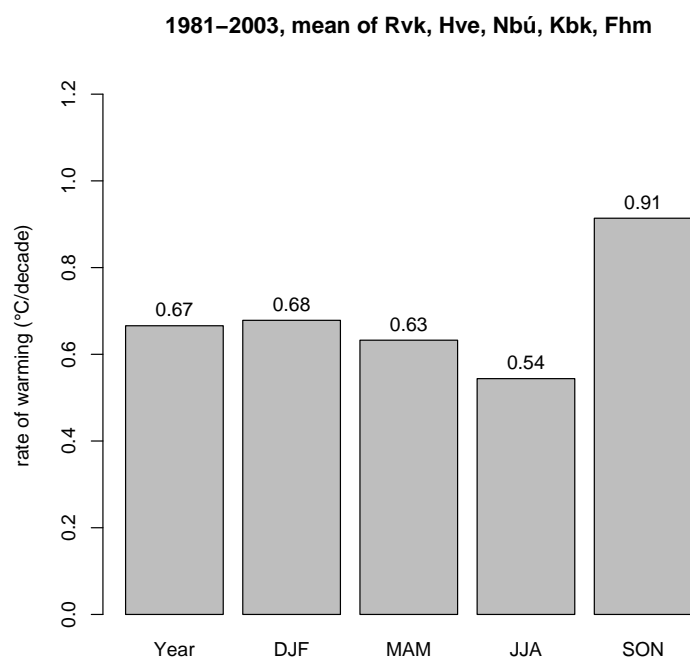


Figure 17: *Average change per decade in the annual and seasonal mean temperature for the period 1981–2004, the average for the meteorological stations at Reykjavík, Hveravellir, Nautabú, Kirkjubæjarklaustur and Fagurhólsmýri.*

section, it was decided to use the climate change scenario from the previous CCEP climate change project (Sæthun *et al.*, 1998; Jóhannesson *et al.*, 1995a) for this purpose. This older scenario has a slightly higher projected rate of annual warming compared with the CWE-NCS scenario, which mostly arises due to a higher projected summer warming.

## 12 Changes in mass balance

An analysis of the transient response of glaciers to climate change requires the use of a mass balance model coupled to a dynamic model. The results of such modeling with the MBT mass balance model coupled to the dynamic ice flow model of Aðalgeirsdóttir (2003) are presented in Jóhannesson *et al.* (2004) and a more detailed description of such results for both Hofsjökull and southern Vatnajökull is in preparation as a part of the reporting of results obtained within the CWE project. In this and the following sections, we will compute the change in mass balance and runoff resulting from a step change in temperature and precipitation without considering changes in the geometry or extent of the ice cap. The validity of this analysis is limited to the near future, say a few decades from now, when the effect of changes in the geometry of the ice cap on the mass balance may be ignored.

A map of the simulated change in mass balance is shown in Figure 18 for a mean annual warming of 1°C with respect to the 1981–2000 baseline period with a seasonality according to the CWE-NCS scenario and a 5% increase in precipitation. As evident from Figure 14, there has already been considerable warming since the period 1981–2000, perhaps on the order of half a degree C, or even more depending on how one interprets the warming trend after 2000. The simulated mass balance change shown in Figure 18 thus corresponds to the expected situation in about two decades, when warming according to the CWE-NCS scenario has added about 0.5°C to the warming that has already occurred now with respect to the 1981–2000 baseline. This period is so short that one may safely ignore changes in the geometry of the ice cap to a first approximation in an analysis of mass balance changes.

Figure 18 shows that the mass balance change is very unevenly distributed over the ice cap. It is concentrated at the lowest elevations near the ice margin where it comes close to  $-1 \text{ m}_{\text{w.e.}} \text{ a}^{-1}$ , but reaches a minimum in absolute value near the summit where it is below  $0.1 \text{ m}_{\text{w.e.}} \text{ a}^{-1}$  in absolute value. This distribution is mainly caused by a much longer melt season at the lowest elevations, but the higher degree-day coefficient for ice compared to snow and the greater importance of refreezing and retention of liquid water in the snow pack at the highest elevations contribute to this pattern too. A notable feature in Figure 18 is the steep increase in (the absolute value of) the mass balance change near the equilibrium line, which is caused by the transition between the accumulation and ablation areas of the ice cap. The irregular variation of the mass balance change near the equilibrium line, which is also evident in Figure 18, is due to the formulation of the degree-day coefficient for a thin layer of snow as a weighted average of the coefficient values for snow and ice. There is little physical basis for the particular implementation of this weighting used in the MBT model, so this feature in the spatial distribution of the mass balance change is not a valid model prediction.

## 13 Static sensitivity of mass balance to climate changes

The sensitivity of the mass balance of glaciers and ice caps to climate changes is an important concept for estimating future global sea level rise that may occur as a consequence of climate warming as mentioned in the Introduction. It is also important as a general measure of the hydrological effect of the changes in the mass balance of glaciated areas due to climate changes. The *static sensitivity* is defined as the ratio of the change of the specific mass balance of the glacier to the magnitude of a small temperature change

$$S_s = \frac{\Delta B}{\Delta T} . \quad (8)$$

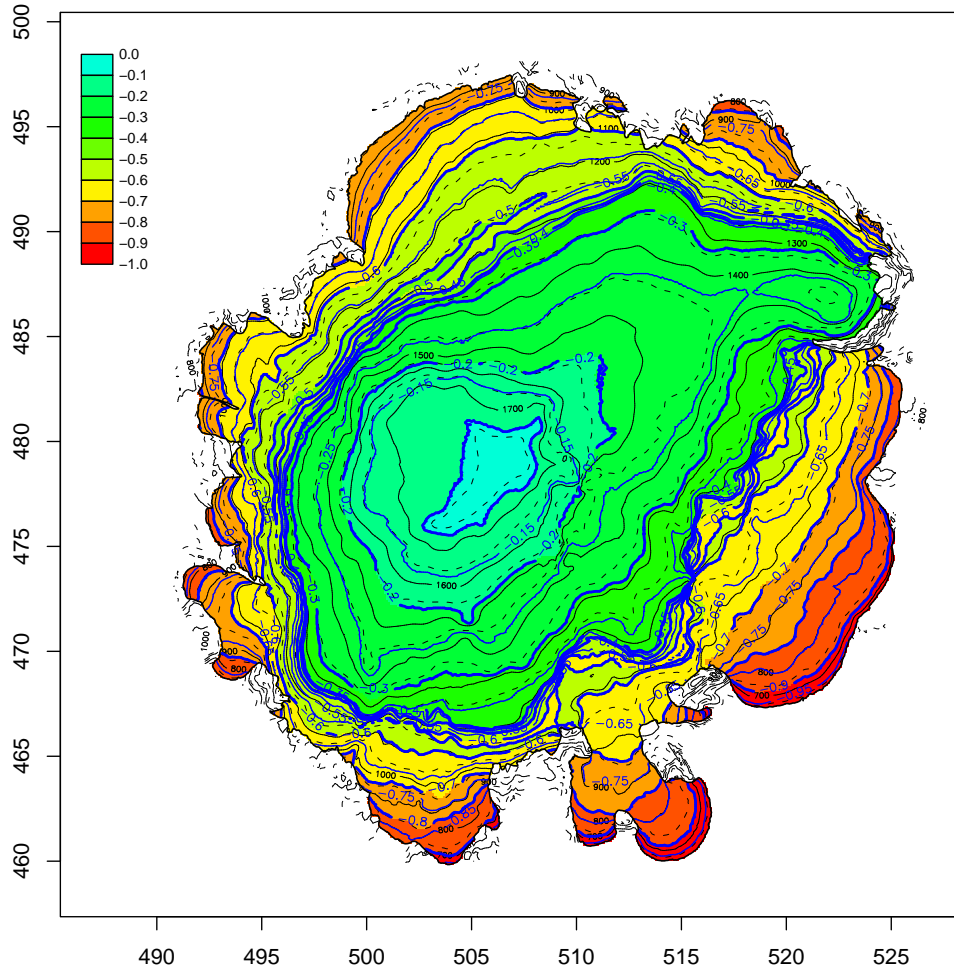


Figure 18: Simulated change in the specific net mass balance of Hofsjökull in  $m_{w.e.} a^{-1}$  (color image and thick blue contours) for a mean annual warming of  $1^{\circ}C$  with a seasonality according to the CWE-NCS scenario and a 5% increase in precipitation per degree of warming (cf. Fig. 11). Thin black contours show the elevation on the ice cap.

Table 5: *Static sensitivity of the mass balance of Hofsjökull ( $m_{w.e.} a^{-1} °C^{-1}$ ) for an annual average warming of  $1°C$  with seasonality according to the CWE-NCS and CCEP temperature scenarios with and without a 5% precipitation increase per degree of warming.*

CWE-NCS $\Delta P=0$	CWE-NCS $\Delta P=5\%$	CCEP $\Delta P=0$	CCEP $\Delta P=5\%$
−0.57	−0.45	−0.67	−0.55

It does not take time-dependent changes in the geometry of the glacier into account. Although the static sensitivity is defined with respect to a small uniform change in temperature it is useful to compute the change in specific mass balance as a consequence of a finite temperature change, which may vary through the year with and without an accompanying precipitation increase as was done in the previous section when the mass balance change corresponding to a  $1°C$  warming was computed. The mass balance sensitivity of Hofsjökull for a warming of  $1°C$  with a seasonality and relative precipitation increase as specified in the four climate scenarios described above is given in Table 5. The sensitivity values in the table are almost the same (within two units in the last digit) as given in Jóhannesson *et al.* (2004), which were based on a model calibration with mass balance data up to the mass balance year 2002/2003. The sensitivity corresponding to the CWE-NCS scenario with  $\Delta P=5\%$  is simply the average over the whole ice cap of the mass balance change shown in Figure 18.

The static sensitivity in Table 5 is similar to previous sensitivity estimates reported by Jóhannesson (1997) for parts of Hofsjökull. It is, however, much lower (in absolute value) than the sensitivity found for Blágnípujökull, Þjorsárjökull and Sátujökull by de Woul and Hock (2006) for a warming of  $1°C$  and no precipitation increase. They estimated sensitivities in the range  $-0.8$  to  $-1.3 m_{w.e.} a^{-1} °C^{-1}$  for these outlet glaciers of Hofsjökull. They assumed a uniform warming within the year, which leads to somewhat higher sensitivity compared with the values computed here corresponding to a sinusoidal seasonal temperature variation with the largest warming during winter. In spite of this, the large difference between their results and the values in Table 5 indicates that something in their simplified approach to mass balance modeling for a large number of glaciers, where average summer and winter balance is computed based on conditions near the ELA, leads to a larger sensitivity than would be found with a more detailed model for the whole elevation range of the glacier. In particular, the sensitivity  $-1.3 m_{w.e.} a^{-1} °C^{-1}$ , which was obtained for Sátujökull by de Woul and Hock, is hard to reconcile with the results obtained here with the MBT model. In this connection, it may be noted that the mass balance model of Hock (1999), with potential radiation and horizontal precipitation gradients, which was mentioned in Section 8, gives results for Hofsjökull that are in good agreements with results obtained here with the MBT model (Thorsteinsson *et al.*, 2006). De Woul *et al.* (2006) also computed the static sensitivity of the whole Hofsjökull ice cap using the mass balance model of Hock (1999), but without horizontal precipitation gradients. They obtained  $-0.95 m_{w.e.} a^{-1} °C^{-1}$  for a uniform temperature increase within the year without a precipitation change. This is somewhat higher than the values corresponding to the CWE-NCS and CCEP scenarios with  $\Delta P = 0$  that are obtained here and given in Table 5, indicating that the assumed seasonality of the temperature change affects the estimated sensitivity considerably.

## 14 Changes in glacial runoff

The change in the mass balance of the ice cap leads to a substantial increase in glacier runoff as seen in Figure 19, which shows monthly average runoff from the whole ice cap for the baseline period, and corresponding to a warming of  $1°C$ , with temperature seasonality and precipitation change according

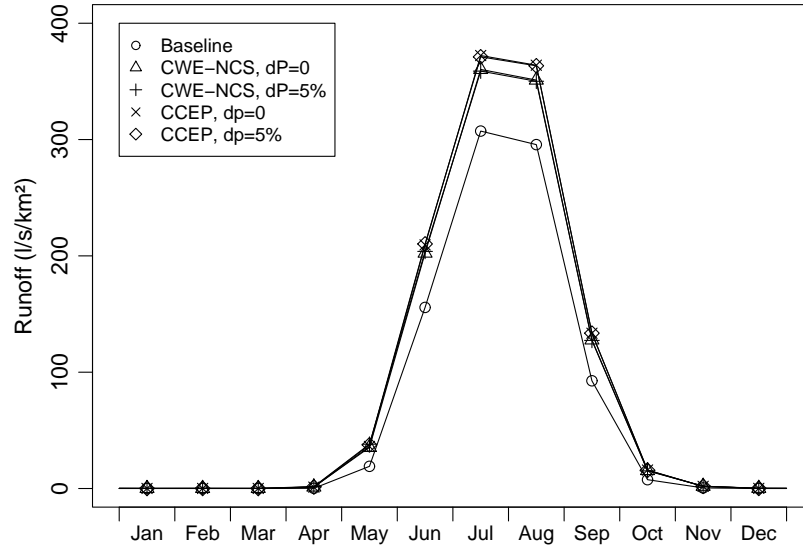


Figure 19: Simulated monthly average runoff from Hofsjökull for the 1981–2000 baseline period and for a warming of 1°C with seasonality according to the CWE-NCS and CCEP temperature scenarios with and without a 5% precipitation increase per degree of warming.

to the four scenarios described above. Only changes in monthly average runoff from the ice surface are considered here and not changes in diurnal runoff characteristics, which may also be important, or routing through firn, basal and groundwater reservoirs, which affects the runoff as it appears in glacial rivers that issue from the ice cap. The runoff change includes a contribution from the change in precipitation on the glacier due to the precipitation change specified by the climate scenario, but this effect is very small as is evident from Figure 19.

The simulated runoff increase shown in Figure 19 reaches a maximum in the middle of the summer, with a somewhat larger increase for the CCEP scenarios compared with the CWE-NCS scenarios as expected, due to a larger summer warming relative to the annual average in the CCEP scenarios. The largest relative changes in the period May to October, when there is runoff to speak of from the ice cap, occur in May and October, when the runoff increases by about a factor of two. The average annual runoff change resulting from a warming of 1°C is according to these results in the range 0.6–0.7 m a<sup>-1</sup>, which is approximately 25% of the current annual average runoff from the ice cap.

The runoff change simulated in this way does not take the dynamic lowering of the ice surface with time into account as mentioned previously. Dynamical modeling with the mass balance model calibrated with data up to the mass balance year 2002/2003, where this effect is taken into account, does, however, lead to very similar results at the point in time when the warming reaches 1°C (Jóhannesson *et al.*, 2004), indicating that this effect is not very important until after that.

## 15 Discussion

The results of the mass balance modeling of Hofsjökull with 16 years of data from the period 1988 to 2004 are in good agreement with the previous results of Jóhannesson *et al.* (1995b). The previous results were found from mass balance modeling of the northern part of the ice cap only and with only four years of data from the period 1988 to 1992. The model calibration derived here was tested by repeated calibration using subsets of the data and found to be relatively stable. This indicates that the results are robust against various details in the formulation and calibration of the mass balance model.

The modeling explains over 80% and 95% of the variance in the winter and summer balance data, respectively. This makes it possible to extrapolate the observations in space and time with some confidence, both to unmeasured parts of the ice cap and also to time periods that start before the measurements. The modeling, furthermore, makes it possible to interpret and analyse unmeasured or partly measured components of the mass balance, including the total precipitation on the ice cap, which opens up new possibilities to use the data in meteorological applications.

The meteorological conditions on Hofsjökull and the other main ice caps in Iceland span a large range of temperature and precipitation due to the large altitude range, which is on the order of 1000 m. Climate conditions in the near future are likely to remain within the already observed range on the glaciers to some approximation, unless the climate changes are so large or rapid that the climate of the region changes in a fundamental way. Thus, parameter values, determined from mass balance observations for the current climate, may be expected to be meaningful for climate change studies to some approximation. Therefore, the results of the modeling of mass balance changes due to possible future climate change, including estimates of the sensitivity of the mass balance to warming, may be expected to be robust.

There is some systematic structure in the mass balance residuals from individual years. The winter balance appears in some cases to have a spatial distribution, which is not captured by the simple precipitation model. This may be due to changes between years in the relative frequency of wind directions that bring precipitation to the ice cap. This could be improved by using a better, physically based precipitation model, based on more detailed meteorological information about the state of the atmosphere over Iceland, for example ERA40 reanalysis data. Systematic errors in the summer balance may be caused by a dependency of the ablation on wind conditions (Guðmundsson *et al.*, 2003), which is not captured by a simple degree-day model. At the moment it seems most fruitful to improve the precipitation model first and to analyse the residuals that remain after such improvements in terms of deficiencies in the melt model.

## 16 Acknowledgements

This study was carried out as a part of the projects *Climate, Water and Energy* (CWE) initiated by the directors of the Nordic Hydrological Institutes (CHIN) with funding from the Nordic Energy Research of the Nordic Council of Ministers, *Climate and Energy* (CE), also financed by Nordic Energy Research, and *Veðurfar, vatn og orka* and *Veðurfar og orka* (VVO, VO) sponsored by the National Power Company of Iceland and the National Energy Fund of Iceland. Trausti Jónsson at the Icelandic Meteorological Office provided the time series of monthly mean temperature in Reykjavík from 1866. The underlying four regional climate projections for the CWE-NCS climate change scenario are provided by the SMHI, the DMI and the met.no. Earlier work on these projections has been supported by the Foundation for Strategic Environmental Research (MISTRA), EU-contracts no. EV5V-CT92-0216 and EV5V-CT94-0505, ELSAM and the Norwegian Research Council.

We thank Philippe Crochet and Trausti Jónsson for constructive comments.

## 17 References

- Aðalgeirsdóttir, G. (2003) Flow dynamics of the Vatnajökull ice cap, Iceland. VAW/ETH Zürich, Mitteilungen no. 181.
- Björnsson, H. (1988) *Hydrology of Ice Caps in Volcanic Regions*. Reykjavík, Societas Scientiarum Islandica, Rit **45**, 139 pp.
- Boville, B. A. and P. R. Gent (1998) The NCAR Climate System Model, Version One. *J. Climate*, **11**, 1115–1130.

- Braithwaite, R. J. (1985) Calculation of degree-days for glacier-climate research. *Z. Gletscherk. Glazialgeol.*, **20**, 1–8.
- Christensen, J. H., J. Räisänen, T. Iversen, D. Bjørge, O. B. Christensen and M. Rummukainen (2001) A synthesis of regional climate change simulations — A Scandinavian perspective. *Geophys. Res. Lett.*, **28**(6), 1003–1006.
- Church, J. A., J. M. Gregory, P. Huybrechts, M. Kuhn, K. Lambeck, M. T. Nhuan, D. Qin and P. L. Woodworth (2001) Changes in sea level. In Houghton, J. T., Y. Ding, D. J. Griggs, M. Noguer, P. J. van der Linden, X. Dai, K. Maskell and C. A. Johnson, eds. *Climate Change 2001: The Scientific Basis. Contribution of Working Group I to the Third Assessment Report of the Intergovernmental Panel on Climate Change*. Cambridge, UK, and New York, NY, USA, Cambridge University Press, 881 pp.
- Curry, R., B. Dickson and I. Yashayaev (2003) A Change in the Freshwater Balance of the Atlantic Ocean over the Past Four Decades. *Nature*, **426**, 826–29.
- de Woul, M. and R. Hock (2006) Static mass balance sensitivity of Arctic glaciers and ice caps using a degree-day approach. *A. Glaciol.*, **42**, in press.
- de Woul, M., R. Hock, M. Braun, Th. Thorsteinsson, T. Jóhannesson and S. Halldórsdóttir (2006) Firn layer effect on glacial runoff—A case study at Hofsjökull, Iceland. *Hydrological Processes*, accepted.
- Einarsson, M. Á. (1976) *Veðurfar á Íslandi*. Reykjavík, Íðunn, 150 pp.
- Eyþórsson, J. and H. Sigtryggsson (1971) The climate and weather of Iceland. In *The Zoology of Iceland*, I(3). Copenhagen and Reykjavík, Ejnar Munksgaard, 62 pp.
- Flato, G. M. and G. J. Boer (2001) Warming Asymmetry in Climate Change Experiments. *Geophys. Res. Lett.*, **28**, 195–198.
- Gordon, C., C. Cooper, C. A. Senior, H. Banks, J. M. Gregory, T. C. Johns, J. F. B. Mitchell and R. A. Wood (2000) The simulation of SST, sea ice extents and ocean heat transports in a version of the Hadley Centre coupled model without flux adjustments. *Climate Dyn.*, **16**, 147–168.
- Guðmundsson, S., H. Björnsson, F. Pálsson and H. H. Haraldsson (2003) *Comparison of physical and regression models of summer ablation on ice caps in Iceland*. Science Institute, University of Iceland, and National Power Company of Iceland, Rep. RH-15-2003.
- Hock, R. (1999) A distributed temperature-index ice- and snowmelt model including potential direct solar radiation. *J. Glaciol.*, **45**(149), 101–111.
- Hock, R., P. Jansson, P. and L. Braun (2005) Modelling the response of mountain glacier discharge to climate warming. In Huber, U. M., H. K. M. Bugmann and M. A. Reasoner, eds. *Global Change and Mountain Regions—A State of Knowledge Overview*. Advances in Global Change Series. Dordrecht, Springer, 243–52.
- IPCC (1990) *Climate change: The IPCC Scientific assessment*. Houghton, J. T., G. J. Jenkins, and J. J. Ephraums, eds. Cambridge University Press, Cambridge, UK, 365 pp.
- IPCC (1996) *Climate change 1995: The Science of Climate Change. Contribution of Working Group I to the Second Assessment Report of the Intergovernmental Panel on Climate Change*. Houghton, J. T., L. G. Meira Filho, B. A. Callander, N. Harris, A. Kattenberg and K. Maskell, eds. Cambridge University Press, Cambridge, UK and New York, NY, USA, 572 pp.
- IPCC (2001) *Climate Change 2001: The Scientific Basis. Contribution of Working Group I to the Third Assessment Report of the Intergovernmental Panel on Climate Change*. Houghton, J. T., Y. Ding, D. J. Griggs, M. Noguer, P. J. van der Linden, X. Dai, K. Maskell and C. A. Johnson, eds. Cambridge University Press, Cambridge, UK, and New York, NY, USA, 881 pp.
- Johns, T. C., R. E. Carnell, J. F. Crossley, J. M. Gregory, J. F. B. Mitchell, C. A. Senior, S. F. B. Tett and R. A. Wood (1997) The Second Hadley Centre coupled ocean-atmosphere GCM: Model description, spinup and validation. *Climate Dyn.*, **13**, 103–134.
- Jóhannesson, T. (1997) The response of two Icelandic glaciers to climatic warming computed with a



- degree-day glacier mass balance model coupled to a dynamic glacier model. *J. Glaciol.*, **43**(143), 321–327.
- Jóhannesson, T. (2003) *Data format for mass balance data and other glacier data in the CWE project*. Reykjavík, Icelandic Meteorological Office, Memo TóJ-2003-04.
- Jóhannesson, T., O. Sigurðsson, T. Laumann and M. Kennett (1993) *Degree-day mass balance modelling with applications to glaciers in Iceland and Norway*. Reykjavík, Nordic Hydrological Programme, NHP-report no. 33.
- Jóhannesson, T., T. Jónsson, E. Källén, E. Kaas (1995a) Climate change scenarios for the Nordic countries. *Climate Res.*, **5**, 181–195.
- Jóhannesson, T., O. Sigurðsson, T. Laumann and M. Kennett (1995b) Degree-day mass balance modelling with applications to glaciers in Iceland, Norway and Greenland. *J. Glaciol.*, **41**(138), 345–358.
- Jóhannesson, T., G. Aðalgeirsdóttir, H. Björnsson, C. E. Bøggild, H. Elvehøy, S. Guðmundsson, R. Hock, P. Holmlund, P. Jansson, F. Pálsson, O. Sigurðsson and P. Þorsteinsson (2004) *The impact of climate change on glaciers in the Nordic countries*. Reykjavík, The CWE Project, Rep. no. 3.
- Knutson, T. R., T. L. Delworth, K. W. Dixon and R. J. Stouffer (1999) Model assessment of regional surface temperature trends (1949–1997). *J. Geophys. Res.*, **104**, 30981–30996.
- Leggett, J. W., J. Pepper and R. J. Swart (1992) Emission scenarios for the IPCC: an update. In Houghton, J. T., B. A. Callander, and S. K. Varney, eds. *Climate Change 1992. The Supplementary Report to the IPCC Scientific Assessment*. Cambridge, UK, and New York, NY, USA, Cambridge University Press, 69–95.
- Nakicenovic, N. and R. Swart (eds.) (2000) *Emissions Scenarios. A Special Report of Working Group III of the Intergovernmental Panel on Climate Change*. Cambridge University Press, UK, 570 pp.
- Obleitner, F. (2000) The energy budget of snow and ice at Breiðamerkurjökull, Vatnajökull, Iceland. *Boundary-Layer Meteorol.*, **97**, 385–410.
- Räisänen, J. (2003) *CWE data documentation*. SMHI/Rosby Centre, Memo, January 2003.
- Räisänen, J., U. Hansson, A. Ullerstig, R. Döscher, L. P. Graham, C. Jones, H. E. M. Meier, P. Samuelsson and U. Willén (2004) European climate in the late twenty-first century: regional simulations with two driving global models and two forcing scenarios. *Climate Dyn.*, **22**, 13–31.
- Reeh, N. (1991) Parameterization of melt rate and surface temperature on the Greenland ice sheet. *Polarforschung*, **59**(3), 113–128.
- Roeckner, E., L. Bengtsson, J. Feichter, J. Lelieveld and H. Rodhe (1999) Transient climate change simulations with a coupled atmosphere-ocean GCM including the tropospheric sulfur cycle. *J. Climate*, **12**, 3004–3032.
- Rummukainen, M., J. Räisänen, D. Bjørge, J. H. Christensen, O. B. Christensen, T. Iversen, K. Jylhä, H. Ólafsson and H. Tuomenvirta (2003) Regional climate scenarios for use in Nordic water resources studies. *Nordic Hydrology*, **34**(5), 399–412.
- Sigurðsson, F. H. (1990) Vandamál við úrkomumælingar á Íslandi. In Sigbjarnarson, G. ed. *Vatnið og Landið, vatnafræðiráðstefna, október 1997*, Reykjavík, Orkustofnun, 101–110.
- Sigurðsson, O. (1989–2004) Afkoma Hofsjökuls 1987–1988, ... 2003–2004 (Mass balance of Hofsjökull 1987–1988, ... 2003–2004). Reykjavík, National Energy Authority. (Technical reports in Icelandic).
- Sælthun, N. R., P. Aittoniemi, S. Bergström, K. Einarsson, T. Jóhannesson, G. Lindström, P.-E. Ohlsson, T. Thomsen, B. Vehviläinen, K. O. Aamodt (1998) *Climate change impact on runoff and hydropower in the Nordic countries—Final report from the project “Climate change and energy production.”* Copenhagen, Nordic Council of Ministers, TemaNord 1998:552.
- Þorsteinsson, Þ., O. Sigurðsson, T. Jóhannesson and G. Larsen (2002) Ice core drilling on the Hofsjökull ice cap. *Jökull*, **51**, 25–41.
- Þorsteinsson, Th., B. E. Einarsson, T. Jóhannesson and R. Hock (2006) *Comparison of degree-day*

*models of the mass balance of the Hofsjökull ice cap.* Reykjavík, National Energy Authority, in press.

Þorsteinsson, Þ., T. Jóhannesson, O. Sigurðsson, E. Ö. Hreinsson, S. Ágústsson and E. Tómasson (2003) *Afkomumælingar á hábungu Hofsjökuls í maí 2003. [Winter balance measurements in the summit area of the Hofsjökull ice cap in May 2003].* Reykjavík, National Energy Authority, Rep. OS-2003/053, 50 pp.

## **A Appendix: Man-pages for the MBT mass balance model**

**NAME**

*mbt*, *tmbt*, *massbxyzt* – degree-day mass balance model for temperate glaciers (v. 2)

**SYNOPSIS**

**tmbt** [options] param-file elev-file temp-file precip/acc-file [pe-file] [int-file]

call **imbt** (sgm,tsn,grt,grp,rko,sko,pko,ddi,dds,sis,rfr, ...

elt,elp,elq,det,dep,dtc,dts,xc0,yc0,pgx,pgy)

call **wcorr** (t,nt,p,cp,np,tms,tc,ts)

call **mbt** (t,nt,p,np,s,l,nel,x,y,nxy,e,ne,ee,pe,npe,r,nr,nv,fd,ld,nfld,xpk,nxpk)

call **rmbt** ()

call **imassbxyzt** (parfile,tparfile,tfile,pfile,tt,ntd,nt,pp,npd,np)

call **massbxyzt** (tt,nt,pp,np,x,y,z,yr,md,m,n,b,c,a,p,r,s,l,w)

**DESCRIPTION**

*tmbt* is a program that computes the mass balance of a temperate glacier as a function of altitude. The program uses the subroutine *mbt* for the mass balance computations. *mbt* can be called by other programs that need to compute glacier mass balance, *e.g.* dynamic glacier models. The subroutines *imbt* and *rmbt* are used in conjunction with *mbt* for parameter initialisation and parameter printing, respectively. The subroutine *wcorr* performs wind correction on measured precipitation. The subroutines *massbxyzt* and *imassbxyzt* provide a calling interface to *mbt* that is suitable for initialisation and repeated calling from within a 2D dynamic glacier model. They may be used to implement a time-dependent climate change with a constant rate of warming.

The model uses temperature and precipitation data (from meteorological stations) in the vicinity of the glacier for the mass balance computations. Temperature and precipitation on the glacier are computed using constant temperature and precipitation gradients with altitude, and, optionally, linear horizontal precipitation gradients. Melting of snow and ice is computed from positive degree-days *PDD* with different degree-day factors for snow and ice. The model can use daily, monthly or yearly precipitation or a snow accumulation directly specified as a function of altitude. The temperature can be specified as a series of daily or monthly mean values, or as a sinusoidal variation in the mean daily temperature as a function of time within the mass balance year with superimposed statistical temperature fluctuations. The model may also be used to fit a least squares sinusoidal function to a record of daily or monthly temperature values, in which case the degree-day computations will be based on this least squares sinusoidal function. The precipitation is assumed to fall as snow if the temperature at the altitude in question is below a specified threshold. If the temperature is given as monthly mean values or specified as a sinusoidal function, the degree-day computations and the determination of the fraction of the precipitation that falls as snow are based on an assumed statistical distribution of the temperature deviation from the monthly mean values or from the assumed sinusoidal function, respectively. A wind correction with separate correction factors for rain and snow, may be applied to the precipitation before it is used in the mass balance computations. Refreezing of melt water and wetting of the snow by melt or rain water are computed as a specified fraction of the remaining snow.

The subroutine *mbt* can compute the mass balance over a specified *interval* within the mass balance year in addition to computing the mass balance of a whole mass balance year. The interval is given in days or months depending on the temperature specification. This feature is used in the program *tmbt* to compute the distribution of the mass balance components within the mass balance year if requested. This can, for example, be useful for investigating how climatic changes affect the distribution of glacier ablation (or runoff from the glacier) within the year and also for calibration of the model using mass balance measurements which are typically performed at the beginning and end of the ablation season.

The subroutine *mbt* is called with a specified initial snow thickness and liquid water content of the snow (see below in the section *CALLING OF MBT*). Both the initial snow thickness and the snow accumulated during each model run are included in the computations of the liquid water content of the snow (see below). *mbt* can therefore compute the mass balance of a given time interval (equal to or shorter than the mass balance year) without considering the previous mass balance history explicitly. Except when the accumulation is directly specified, the program *tmbt* initialises the snow thickness at the beginning of the mass balance

year by making a preliminary call to *mbt* with zero snow thickness and liquid water content. The initial snow thickness in the actual mass balance computation is put equal to the snow thickness found in this preliminary integration up to a maximum of 0.5 m water equivalent. When the accumulation is given directly, the initial snow depth is put equal to the specified accumulation and the precipitation is put equal to zero. The liquid water content at the beginning of the mass balance year is then specified as zero. This somewhat arbitrary initialisation results in a realistic division of the glacier into an accumulation and an ablation area at the beginning of the mass balance year. Other programs that use the subroutine *mbt* are free to use other strategies for the specification of the initial snow thickness and liquid water content.

## STATISTICAL DISTRIBUTION OF TEMPERATURE VARIATIONS

A statistical approach is used in the determination of positive degree-days and the fraction of the precipitation that falls as snow when the temperature is specified as monthly mean values or as a sinusoidal function. Temperature deviations from the monthly means or from the sinusoidal function are assumed to be normally distributed with standard deviation  $\sigma$ .

When temperature is specified as daily values, the positive degree-days and the fraction of the precipitation that falls as snow are computed directly from the daily values without any statistical considerations.

### Monthly temperature values

Assuming a uniform distribution of the precipitation within each month or that precipitation and temperature fluctuations within the month are uncorrelated, the fraction  $f$  of the precipitation that falls as snow during the month can be computed as

$$f = \frac{1}{\sigma\sqrt{2\pi}} \int_{-\infty}^{T_s} e^{-(T-T_m)^2/(2\sigma^2)} dT$$

$$= \frac{1}{2} \operatorname{erfc}(-(T_s - T_m)/(\sqrt{2}\sigma)) , \quad (1)$$

where  $T$  is temperature,  $T_s$  is a threshold (typically about 1°C),  $T_m$  is the monthly mean temperature and  $\operatorname{erfc}$  is the complementary error function

$$\operatorname{erfc}(x) = \frac{2}{\sqrt{\pi}} \int_x^{\infty} e^{-\xi^2} d\xi . \quad (2)$$

Distributing the days of the year evenly among the months for simplicity, the positive degree-days  $PDD$  in a given month are similarly computed as

$$PDD = \frac{365/12}{\sigma\sqrt{2\pi}} \int_0^{\infty} T e^{-(T-T_m)^2/(2\sigma^2)} dT$$

$$= 365/12 \left( \frac{\sigma}{\sqrt{2\pi}} e^{-T_m^2/(2\sigma^2)} + \frac{1}{2} T_m \operatorname{erfc}(-T_m/(\sqrt{2}\sigma)) \right) . \quad (3)$$

### Sinusoidal temperature variation

If the variation in the mean daily temperature  $T_d$  is assumed to be sinusoidal within the mass balance year then  $T_d$  can be expressed as

$$T_d(t) = T_a + T_{co} \cos(2\pi t/A) + T_{si} \sin(2\pi t/A), \quad (4)$$

where  $t$  is time since the beginning of the mass balance year (in days),  $A$  is the length of the year (in days),  $T_a$  is the average temperature of the year and  $T_{co}$  and  $T_{si}$  are coefficients. Assuming a uniform distribution of the precipitation within the mass balance year or that precipitation and temperature variations within the year are uncorrelated, the fraction of the precipitation that falls as snow in a given time period from day  $D_1$  to day  $D_2$  is given as

$$f = \frac{1}{D} \int_{D_1-1}^{D_2} \frac{1}{\sigma\sqrt{2\pi}} \int_{-\infty}^{T_s} e^{-(T-T_d(t))^2/(2\sigma^2)} dT dt$$

$$= \frac{1}{2D} \int_{D_1-1}^{D_2} \text{erfc}(-(T_s - T_d(t))/(\sqrt{2}\sigma)) dt, \quad (5)$$

where  $D = D_2 - D_1 + 1$  is the period length in days. The positive degree-days in a given year are similarly computed as

$$\begin{aligned} PDD &= \int_{D_1-1}^{D_2} \frac{1}{\sigma\sqrt{2\pi}} \int_0^\infty T e^{-(T-T_d(t))^2/(2\sigma^2)} dT dt \\ &= \int_{D_1-1}^{D_2} \left( \frac{\sigma}{\sqrt{2\pi}} e^{-T_d^2(t)/(2\sigma^2)} + \frac{1}{2} T_d(t) \text{erfc}(-T_d(t)/(\sqrt{2}\sigma)) \right) dt. \end{aligned} \quad (6)$$

Equations (5) and (6) can be evaluated efficiently by traditional algorithms for numerical integration, *e.g.* Simpsons rule.

### OPTIONS OF TMBT

- a** The snow accumulation is directly specified as a function of altitude in an accumulation-file instead of a precipitation-file. The name of the accumulation-file is specified in the same location of the command line as the precipitation-file.
- x** Spatial coordinates  $x$  and  $y$  are specified in the elevation-file in addition to the altitude  $z$  (the file then has three columns instead of only one). This makes it possible to specify explicit locations on the glacier in case the mass balance is not only considered as a function of altitude. This option can be used to specify the locations of mass balance stakes where the mass balance is to be computed.
- s** Locations, elevations and dates of fall, spring and fall measurements are given in the multi-columns format (wsy-format) described in the CWE-memo about mass balance data format (10 columns giving stake-name,  $x$ ,  $y$ ,  $z$ ,  $wbl$ ,  $sbl$ ,  $ybl$ ,  $d0$ ,  $d1$ ,  $d2$ ).
- t** Use the dates specified in a wsy-format elevation/location-file to compute the mass balance of sub-intervals, rather than the default (whole year) or the dates read from an interval-file. The initial day of the computations will then be the first day *after* the fall visit to the glacier and separate mass balance computations will be performed for the winter and summer seasons. The winter and summer seasons extend from  $d0+1$  to  $d1$  and from  $d1+1$  to  $d2$  where  $d0$ ,  $d1$  and  $d2$  are the dates given in the three last columns of the wsy-file.
- j** Jump over the first date in the interval-file without performing mass balance computations for the interval 1 to  $d1$ , where  $d1$  is the first date in the file. Then the mass balance computations will be started on day ( $d1+1$ ).
- f** Fit mass balance data in wsy-format elevation/location-file by adjusting the precipitation correction  $pko$  so that the appropriate mass balance components are reproduced. This fitting is only carried out for years/seasons where the corresponding mass balance is positive. The whole year and the winter and summer seasons are fitted independently so that the sum of the modelled winter/summer precipitation and some of the mass balance components may not equal the corresponding yearly precipitation or yearly component. The sum of the winter and summer model results is written out separately and can thus be compared to the fitted yearly values. The fitting procedure is implemented as a simple loop which sometimes does not produce accurate results when the mass balance is near zero. Such results are not automatically recognised by the program and must be identified by the user. This option should therefore be used with caution and the resulting fitted mass balance compared with the original measured mass balance. The fitting has succeeded then they are equal or almost equal, but the fitting procedure may fail in case the mass balance is near zero and then the results of the fitting are of little use.

- w** Use wide output format for model results (print with stake-name, x, y at the start of each line of output).
- W** Use output format where intervals from wsy-file are printed at the end of the output lines.
- d** Use double precision format for model results and model parameters. This is useful for optimal parameter fitting (intended for programming purposes where the full numerical accuracy of the results is needed).
- F, -n** Fitting options (see code).
- v** Print program version on stderr and exit.
- [-h|-H|-?]** Print help text on stderr and exit.

## INPUT TO TMBT

The input to *tmbt* is read from files with names which are given as command line parameters.

- param-file** Various computational parameters. Each line specifies one parameter and consists of the value of the parameter as a floating point number followed by the three letter name of the parameter. The parameter value and the parameter name are separated by a space or a tab. The parameter names are the same as the names of the arguments in the call of the subroutine *imbt* as shown in the *SYNOPSIS* section above. All of the first 16 parameters must be specified although some of them may not actually be used in all cases. Optional parameters may be used to specify horizontal precipitation variations and a seasonal variation of a climatic temperature change. The parameters are described below in a separate section.
- elev-file** Elevation file. The mass balance is computed at a number of elevations (*ne*) specified by this file. The elevations may either be specified as a list of discrete elevation values (*ne*=1 or *ne*>3) or as three values which specify a minimum elevation, an elevation increment and a maximum elevation, respectively. If the option *-x* is given (see above) then this file is assumed to contain *x*, *y*, *z* values in three columns. If the option *-s* is given (see above) then this file is assumed to be in the wsy-format described in the CWE-memo about mass balance data format (10 columns giving stake-name, *x*, *y*, *z*, *wbl*, *sbl*, *ybl*, *d0*, *d1*, *d2*).
- temp-file** Temperature file/files. If more than one file needs to be specified, all the names are given as one command line argument where the individual names are separated by commas (",") without spaces between the names. The number of values in the file/files (*nt*) determines whether the values are daily mean values ( $150 \leq nt \leq 1000$ ), monthly mean values ( $6 \leq nt \leq 24$ ) or parameters specifying a sinusoidal variation in the mean daily temperature within mass balance year ( $nt=2,3$ ). If a sinusoidal variation is used then the values in the file specify the mean temperature  $T_a$ , and the coefficients  $T_{co}$  and  $T_{si}$  corresponding to the cosine and sine terms in the sinusoidal function (cf. equation (4) above). The sine coefficient  $T_{si}$ , may be omitted in which case it is assumed to be zero. It is not possible to compute the mass balance for shorter periods than one mass balance year if  $T_{si}$  is omitted because then the phase of the temperature variation is likely to be meaningless. In that case, all the accumulation is deposited on the surface of the glacier before the melting starts. Otherwise, accumulation and melting occur simultaneously through the mass balance year such that melting during the late fall (*i.e.* after the beginning of a new mass balance year) in the ablation area of the glacier is according to the degree-day factor for ice. The number of values in the temperature file can be different from the number of days (months) in a calendar year if the user wishes to model a mass balance year which is longer or shorter than a calendar year (this may occur in practice if mass balance measurements are carried out on different dates in different years).
- precip/acc-file** Precipitation file/files. If more than one file needs to be specified, all the names are given as one command line argument where the individual names are separated by commas (",") without spaces between the names. The number of values in the file/files (*np*) determines whether the values are daily precipitation ( $150 \leq nt \leq 1000$ ), monthly precipitation ( $6 \leq nt \leq 24$ ) or yearly precipitation (*np*=1). If *np* is not equal to 1 then *np* must be equal to *nt*.

If the  $-a$  option is given then this file specifies the snow accumulation directly instead of computing it from the precipitation. The accumulation is then given as one value for each elevation for which the mass balance is to be computed. The mass balance can only be computed for a whole year if the accumulations is specified in this way. No wind correction is applied to the accumulation read from an accumulation file and the climatic precipitation increase specified by the parameter *dep* (see below) does not apply to accumulation specified in this way. This option is primarily useful for calibration purposes.

**precip-elev-file**

File describing the relative variation of precipitation with elevation. This optional file is specified on the command line if the parameter *grp* in *par-file* is given as -1.0. Then the parameters *rko*, *ske* and *pko* are used as before to compute the precipitation at the elevation *elq*, which is assumed to be within the elevation range of the glacier. The precipitation at other elevations on the glacier is assumed to be in the same proportion to the precipitation at *elq* as specified by the data in the *precip-elev-file*. Linear interpolation is used to compute values in between the pairs of *z* and *p* that are given in the file.

**int-file**

Interval file. If this optional file is specified on the command line then the mass balance is computed for given intervals within the mass balance year. The (whole) numbers in the file (one per line) are interpreted as months if  $6 \leq nt \leq 24$ , but as days otherwise. If the mass balance is computed in this way, it is critical that the temperature and precipitation records start at the beginning of the mass balance year, if daily or monthly values are used, and that the phase of the sinusoidal temperature variation within the year is properly specified, if the temperature variation is specified in that way. In the case of sinusoidal temperature variation, the phase is determined by the sign and the relative importance of the coefficients  $T_{co}$  and  $T_{si}$ . If  $T_{si}$  is omitted from the specification of the sinusoidal function then it is not possible to compute the mass balance of intervals shorter than one year. The section *OUTPUT FROM TMBT* below describes the output, when the optional *int-file* is specified, in more detail. The *int-file* may also be used to limit the mass balance computations (the mass balance year) to a shorter period than the number of days or months given by *nt*. In that case the *int-file* will contain only one value which is the last day or month of the mass balance year. This option simplifies the preparation of input files for *tmbt* in some cases. Dates in the *int-file* may also be specified as calendar days in the format 'aaaammdd'. Then the data files must start on 1 January of the initial year of the mass balance year. The first date in the *int-file* may be given as a negative number in order to specify an initial day for the mass balance computations. Temperature and precipitation data before this day are then ignored and the mass balance computations are started on the specified day. The initial day of the computations should, as a rule, be specified as the day after the fall visit to the glacier. This is primarily useful when data files correspond to calendar years and dates in *int-file* are specified as calendar days. The *-j* option may also be used to jump over a specified time period in the beginning of the data files. If the *-j* option is given, the mass balance computations will be started on day (*d1*+1) where *d1* is the first date in the file.

The parameters that need to be specified in the parameter file are described below. An example value for each parameter with units where applicable is given after a short description of the parameter.

- sgm** standard deviation of temperature deviations from the monthly mean values or from a sinusoidal function. If *sgm* is specified as a negative number then a temperature record of monthly or daily temperature values will be used for computing a least squares sinusoidal temperature variation within the mass balance year and the sinusoidal function together with the (absolute) value of *sgm* will be used for the computation of degree days. The computation of the fraction of the precipitation that falls as snow is not affected by a negative value of *sgm*. Example: 3.0 (°C).
- tsn** snow/rain threshold. Example: 1.0 (°C).
- grt** temperature/elevation gradient, positive value of the parameter specifies decreasing temperature with elevation. Example: 0.6 (°C/100m).



<b>grp</b>	precipitation/elevation gradient. Example: 0.1 (1/100m).
<b>rko</b>	rain correction factor for measured precipitation > 1. Example: 1.2.
<b>sko</b>	snow correction factor for measured precipitation > 1. Example: 1.8.
<b>pko</b>	precipitation correction factor for measured precipitation. The precipitation correction factor represents the relation between the measured precipitation at the precipitation station and the precipitation at elevation <i>elq</i> on the glacier ( <i>cf.</i> the formula in the description of the parameter <i>elq</i> below). Example: 1.0.
<b>ddi</b>	degree-day factor for ice. Example: 0.006 (m <sub>w.e.</sub> /°C/day).
<b>dds</b>	degree-day factor for snow. Example: 0.004 (m <sub>w.e.</sub> /°C/day).
<b>sis</b>	snow thickness for blending of <i>ddi</i> and <i>dds</i> . Example: 0.3 (m <sub>w.e.</sub> ).
<b>rfr</b>	refreezing ratio, the relative amount of liquid or refrozen water (either melt water or rain) stored in the snow must exceed <i>rfr</i> before runoff occurs. Example: 0.07.
<b>elt</b>	elevation of temperature station. Example: 700 (m a.s.l.).
<b>elp</b>	elevation of precipitation station. Example: 700 (m a.s.l.).
<b>elq</b>	starting elevation for the precipitation gradient computations. The precipitation at an elevation <i>e</i> is computed according to the formula $p_{ko} \cdot p_m(1 + (e - elq)grp/100)$ , where $p_m$ is the corrected measured precipitation at the precipitation station. Example: 700 (m a.s.l.).
<b>det</b>	temperature change, for example climatic warming. A seasonal variation in the temperature change may be introduced with the parameters <i>dtc</i> and <i>dts</i> that are described below. Example: 2.0 (°C).
<b>dep</b>	relative precipitation increase per degree of temperature change. The precipitation is multiplied by $(1 + dep)^{det}$ if a <i>dep</i> value different from zero is specified. Example: 0.05 (1/°C).
<b>dtc</b>	coefficient of an optional cosine seasonal term in the temperature change. Example: 0.0 (°C).
<b>dts</b>	coefficient of an optional sine seasonal term in the temperature change. Example: 0.0 (°C).
<b>xc0</b>	x-coordinate of the origin of a bilinear spatial precipitation distribution. Example: 500000.0 (m).
<b>yc0</b>	y-coordinate of the origin of a bilinear spatial precipitation distribution. Example: 500000.0 (m).
<b>pgx</b>	spatial precipitation gradient in the x-direction. Example: 0.02 (1/1000m).
<b>pgy</b>	spatial precipitation gradient in the y-direction. Example: -0.02 (1/1000m).

The parameters *xc0*, *yc0*, *pgx* and *pgy* can be used to specify a linear precipitation variation in 2 horizontal directions. If a more complicated precipitation variation is needed, the subroutine *xyz(x,y,z)*, defined in the file *xyz.f* may be redefined in order to implement an arbitrary variation of the precipitation with *x*, *y* and/or *z*.

## OUTPUT FROM TMBT

The output from *tmbt* is written to *stdout* and must be redirected to a file if it needs to be saved on disk. It consists of a header which contains the command line which was used to invoke *tmbt*, the number of values read from the temperature, precipitation and elevation files, the first and last day of the mass balance year (they are equal to zero if a *int-file* is not used), the values of the parameters read from the parameter file and a line of names for the columns that follow.

Below the header the output consists of one line for each elevation for which the mass balance was computed. The lines contain the elevation [m a.s.l.], the positive degree-days [°C day], precipitation, accumulation, ablation, melting of ice, melting of snow, refreezing and mass balance [m<sub>w.e.</sub>]. If the *-w* option is used to specify wide output format, the stake name, and the horizontal coordinates *x* and *y* are also printed out at the start of each line before the elevation (see above). The *accumulation* is the sum of the computed snow-fall. Refrozen rain water (in the rare case when melting is less than needed to wet the snow) is not counted

with the accumulation. Rather it leads to a positive ablation. The *melting* of snow and ice are positive quantities which are found from the computed degree-days. The *refreezing* is a positive quantity for yearly mass balance computations. It is computed as a certain fraction (specified by the parameter *rfr*) of the remaining snow. It denotes both refrozen and stored liquid water (melt water or rain) which does not leave the snow pack either because it is refrozen due to sub-zero temperatures in the snow pack in late winter or early summer, or because a snow pack at the melting point can store some water in liquid form (on the order of 5% by weight). The *refreezing* is always smaller than the sum of the melting and the amount of precipitation that falls as rain. The *refreezing* may sometimes be negative (meaning that liquid water is released from the snow pack) when the mass balance is computed for intervals shorter than one year (see below) because the amount of refrozen or retained liquid water will be reduced during the summer when the thickness of the snow pack is reduced by melting. The *ablation* is defined as the negative of the melting plus the refreezing. It can become positive in the rare case when the refreezing is greater than the melting. The *mass balance* is the sum of the accumulation and the ablation.

Mass balance can be computed for specified *intervals* within the mass balance year by including an *int-file*. In this case the output starts with the same information as for whole year computations, including the results for the yearly balance as described above. Below this output there will be one section for each *interval* in the same format as the whole year results. For example, if the temperature is specified as monthly values and if the *int-file* contains the numbers 3, 6, 9 and 12, then four such sections will be written out. The sections contain mass balance information for four consecutive 3-month intervals from the beginning of the mass balance year. Each section is preceded by a line that specifies the time interval in question. If intervals are specified in this way it is assumed that the mass balance year ends on the last date specified in *int-file* and temperature and precipitation data beyond this date in *t-file* and *p-file* are ignored.

If the accumulation is directly specified through an accumulation file then the precipitation column in the output of *tmbt* contains zeros.

## CALLING OF MBT

The mass balance computations of *tmbt* can be performed by other programs by calling the subroutines *mbt* and *wcorr* directly.

Before *mbt* or *wcorr* are called for the first time, the parameter initialisation subroutine *imbt* must be called. The names and meaning of the parameters in the argument list of *imbt* are the same as described above for the parameters of *tmbt*. The wind correction routine *wcorr*, should be called once after *imbt* has been called and before the first call to *mbt*. The reason that *wcorr* is not called automatically by *mbt* is that *mbt* is typically called repeatedly, but *wcorr* only needs to be called once for a particular set of temperature and precipitation data. The routine *mbt* can then be called once, if whole year results are requested, or repeatedly for consecutive intervals within the mass balance year, if the distribution of the mass balance within the year is to be found.

The argument list of *mbt* specifies the temperature and precipitation in the arrays *t* and *p*, which have the lengths *nt* and *np* respectively, and are interpreted in the same way as described above for the input files *temp-file* and *precip-file* of the program *tmbt*. Two arrays *s* and *l*, which are both of length *nel*, where *nel* is the number of elevations for which the computations are performed, give the thickness of the snow cover and the amount of liquid or refrozen water stored in the snow at the beginning of the time interval for which the mass balance is to be found. Both *s* and *l* are given in m<sub>w.e.</sub>. The subroutine *mbt* does not make any assumptions about the initial snow depth or the liquid water content of the snow at the beginning of the mass balance year and expects the calling program to take care of this by proper initialisation of the arrays *s* and *l*. This provides for flexibility and efficiency in the use of *mbt* which can be used to compute the mass balance for any time period of the mass balance year without considering the previous mass balance history explicitly. If *mbt* is called repeatedly then the calling program must use the returned results of each call to *mbt* to update the arrays *s* and *l* as appropriate before the next call to *mbt* is made. For details, see the source code of *tmbt*. The arrays *x,y*, of length *nxy*, contain the spatial coordinates of the locations where the mass balance will be computed in case spatial coordinates are used. In this case *nxy=nel*. Else the length *nxy=0*. The array *e*, which has length *ne*, specifies the elevations for which the mass balance is computed. The elevations may either be specified as a list of discrete elevation values (*ne=1* or *ne>2*) or as two values which specify a minimum elevation and an elevation increment, respectively. Note that this elevation speci-

fication is slightly different from the specification of elevations with the input file *elev-file* to the program *tmbt* as described above. The reason is that the number of elevations is already given in the argument *nel* and therefore the maximum elevation does not need to be given in the array *e*. A piecewise variation of the precipitation with elevation may be specified with the arrays *ee* and *pe*, of length *npe*, as described above for the input file *precip-elev-file* of the program *tmbt*. An extra precipitation correction may be specified in the array *xpk*. This correction is not used if the length of this array *n timer* *xpk* = 0. Otherwise, the array specifies a separate precipitation correction factor for each point where the mass balance is to be computed. This option is only intended to be used when observed mass balance data are fitted by adjusting the precipitation correction so that the measured mass balance at each point is reproduced (see the *-f* option of *tmbt* that is described above).

The results are returned in the 2D array *r(nr,nv)*. The first defining dimension *nr*, corresponds to the elevations for which the mass balance computations are done and must be greater than or equal to the number of elevations *nel*. The second dimension *nv* is the number of output variables which is requested. The subarrays *r(\*,i)*, *i* = 1, 2, ..., *nv*, contain the mass balance, accumulation, ablation, melting of ice, melting of snow and refreezing [*m<sub>w.e.</sub>*], positive degree-days [°C day] and the precipitation [*m<sub>w.e.</sub>*] (in this order). If *nv* < 8 then one or more of the last subarrays is not returned.

The interval of the computations is specified with the integer arguments *fd* and *ld*. If both *fd* and *ld* are equal to zero then the mass balance computations are performed for a whole mass balance year (*i.e.* for *nt* number of days or months if *nt* > 3). If *fd* and *ld* are different from zero and monthly temperatures are used then the mass balance computations are performed from month *fd* to month *ld*, otherwise the computations are performed from day *fd* to day *ld*. Both *fd* and *ld* may be arrays specifying different intervals for the different elevations for which the mass balance will be computed. In that case, the argument *n timer* *fld* is specified equal to *nel*. Otherwise, *n timer* *fld* is specified as 1.

The subroutine *rm timer* *bt* can be used to write all parameter values set by *im timer* *bt* together with some other relevant information to *stdout*.

An example section from a main program using *im timer* *bt*, *mb timer* *bt* and *rm timer* *bt* is listed below.

```
...
call im timer
      (sgm,tsn,grt,grp,rko,sko,pko,ddi,dds,sis,rfr, ...
      elt,elp,elq,det,dep,dtc,dts,xc0,yc0,pgx,pgy)
call wcorr(t,nt,p,cp,np,tms,tc,ts)
call mb timer
      (t,nt,p,np,s,l,nel,x,y,nxy,e,ne, ...
      ee,pe,npe,r,nr,nv,fd,ld,n timer
      fld)
call rm timer
      bt()
...
```

## CALLING OF MASSBXYZT

The computations of the routine *massbxyz timer* *t* are initialised with one call to *im timer* *massbxyz timer* *t* where model parameters, the rate of climate change and a datum seasonal variation of temperature and precipitation are read from input files. The routine *massbxyz timer* *t* may then be repeatedly called to compute glacier mass balance components as a function of space and time. The routine returns the mass balance, accumulation, ablation (-melting (ice and snow) + refreezing), precipitation and run-off for a whole mass balance year in separate two-dimensional arrays. The climate change within each mass balance year is assumed to be the same. It is computed from time 0.0 to the middle of the corresponding year. There is no climate change before time 0.0. If *massbxyz timer* *t* is called repeatedly within the same mass balance year, it will compute the mass balance only once and return the same results without repeating the computations as long as the given mass balance year is the same. The last model results are *not stored* internally in the subroutine and must therefore be provided in the appropriate output variables on each call (that is the routine does nothing if the mass balance year is the same as in the previous call).

An example section from a main program using *im timer* *massbxyz timer* *t* and *massbxyz timer* *t* is listed below.

```
...
call im timer
      massbxyz timer
      (parfile,tparfile,tfile,pfile,tt,ntp,nt,pp,ntp,np)
```

```

do i=1,nloop
...
call massbxyz(t,nt,pp,np,x,y,z,yr,md,m,n,b,c,a,p,r,s,l,w)
...
yr = yr+dt
end do
...

```

The user must inspect the source code of the routines in order to obtain detailed information regarding the specification of input arrays and work arrays.

## INSTALLATION AND PORTABILITY

*mbt* and *tmbt* are written in *Fortran* for *UNIX* computers. The source code, which has been tested on Linux (v. 2.4.18, Redhat 8.0 distribution), an HP9000 (HP-UX, v. 11) a Sun SPARC (SunOS, v. 5.8) and DEC/Alpha (OSF1, v. 4.0), should compile on most *UNIX* computers with essentially no changes (see comments in the makefile for changes needed on the abovementioned platforms). The source code is distributed as a *shell archive* in two files which are unbundled with the commands

```

sh mbt.dist
sh lnx.dist

```

where *mbt.dist* and *lnx.dist* are the names of the source code distribution files. *mbt.dist* contains the *Fortran* source code and input for tests of the mass balance model and *lnx.dist* contains output from the tests obtained on a Linux machine. The user should be located in a suitable empty directory when she unbundles the source and must make sure that the current directory (".") is in the PATH. The distribution contains a *make* file which describes the compilation and linking of the program *tmbt* and two test programs. The user should read the makefile carefully and make the recommended changes for the platform where the software is being installed.

On *UNIX* computers the command

```
make [> LOG]
```

sets the file permission of a few files, compiles the *Fortran* source code of *tmbt* and the test programs, executes the test programs and a number of test runs of *tmbt* and compares the output of the tests with the expected output (obtained on Linux). NOTE: The definitions of the variables *FC*, *FFLAGS* and *LFLAGS* in the *make* file may not be applicable to all *UNIX Fortran* compilers (the makefile is for the *ifc* Intel compiler on Linux and contains the appropriate definitions for HP, Sun and DEC/Alpha in commented lines). In case of problems try removing the flags *-u* (all variables are implicitly undeclared) or *-O* (full optimisation) or both from the definition of *FFLAGS*. The file *derfc.f* is machine dependent and needs to be adapted to the platform by commenting/uncommenting the appropriate lines and the file *fm\_atof.c* needs to be modified slightly on HP in the same manner (see comments at the beginning of the files).

If all tests run as they should the output should contain a line saying

The files *file1* and *file2* are identical

for each test (in addition to a number of other diagnostic lines from the compiler and the *make* command). In many cases some harmless differences caused by compiler dependent formatting of floating point numbers will be found (e.g. ".12345" versus "0.12345") or precision related differences in the last digit of the output numbers. The output can, if desired, be redirected to a log file for later examination. The *make* command removes object files and the test program executables before exiting, but leaves the *tmbt* executable on the disk. The *make cleanout* command removes the output files from the tests from the disk. In case of problems, the user can make the individual test programs and *tmbt* manually and run the tests, one at a time, by giving the appropriate *make* commands (see the *make* file for details).

The source code of *mbt* and *tmbt* contains no calls to plotting software. All user input is through standard *Fortran* file I/O. All output is written to *stdout* and error messages are written to *stderr*. The code should therefore be easily portable to most non-*UNIX* computers with a *Fortran* compiler.

The output from the program *tmbt* needs to be postprocessed by appropriate plotting software in order to

generate a visual representation of the output. This software will be platform dependent. On *UNIX* computers the utilities *grep(1)*, *awk(1)* and *sed(1)* will be found useful for the processing of the output from *mbt*.

## NOTES AND WARNINGS

Note that the standard deviation of the temperature deviations  $\sigma$ , does not have exactly the same physical meaning for monthly temperature values as for a sinusoidal temperature variation.

Refrozen melt water and the liquid water content of the snow are not distinguished, and the refrozen melt water is released as the snow thickness is reduced by melting in the same way as liquid water stored in the snow.

Checking of input data is not extensive. For example, the user must specify the options *-x* (xy-values given in elevation-file) or *-s* (wsy-formatted elevation-file) correctly. Otherwise, the input data will be incorrectly interpreted, leading to unpredictable results of the computations. Also, care must be taken to use correct units ( $^{\circ}\text{C}$  and  $\text{m}_{\text{w.e.}}$ ) for the input data.

The computation of the yearly mass balance by *mbt* is relatively efficient, especially when the temperature is specified as a mean value and the amplitude of a sinusoidal function ( $nt=2$ ), and the routine is suitable for repeated calling by a dynamic glacier model for this reason. The computation of the distribution of the mass balance within the mass balance year requires somewhat more computational resources.

## AUTHORS AND ACKNOWLEDGEMENTS

The programming of version 1 was carried out by Tómas Jóhannesson in August 1992 at the National Energy Authority in Iceland based on a computer program by Niels Reeh and Tron Laumann. Version 2 was made in 2003 at the Icelandic Meteorological Office. The mass balance model is based on previous work by Roger Braithwaite, Niels Reeh and Tron Laumann.

The source code in *erfc.f*, which evaluates the complementary error function, is written by W. Fullerton. It was obtained from a public domain special functions library from the Los Alamos scientific laboratory.

The modifications introduced in version 2 of the model in 2003 were carried out as a part of the projects CWE and VVO ("Climate, Water and Energy" and "Veðurfar, vatn og orka") that were financed by the Nordic Council of Ministers, the Icelandic Energy Fund and the National Power Company of Iceland.

## REFERENCES

Further information about mass balance modelling using *mbt* may be found in following reports and papers.

Jóhannesson, T. 1997. The response of two Icelandic glaciers to climatic warming computed with a degree-day glacier mass balance model coupled to a dynamic glacier model. *Journal of Glaciology*, **43**, 143, 321-327.

Jóhannesson, T., O. Sigurðsson, T. Laumann and M. Kennett. 1995. Degree-day mass balance modelling with applications to glaciers in Iceland, Norway and Greenland. *Journal of Glaciology*, **41**, 138, 345-358.

Jóhannesson, T., O. Sigurðsson, T. Laumann and M. Kennett. 1993. *Degree-day mass balance modelling with applications to glaciers in Iceland and Norway*. NHP-rapport no. 33, Nordic Hydrological Programme, Reykjavík.

Tómas Jóhannesson. 1993. *Application of a Degree-Day Mass Balance Model to the Qamanârssûp Sermia Outlet Glacier, West Greenland*. OS-93078/VOD-14B, Orkustofnun, Reykjavík.

## AVAILABILITY

The *mbt* software can be obtained from

Tómas Jóhannesson  
 Veðurstofa Íslands — Icelandic Meteorological Office  
 Bústaðavegi 9  
 IS-150 Reykjavík  
 Iceland  
 Phone: +354-1-5226000, Fax: +354-1-5226001, E-mail: tj@vedur.is